

2

AWS/TR-90/001

THIS IS A COPY

AD-A231 567



# CONVECTIVE SCALE DYNAMICS

by

Capt Jeffrey R. Hedges  
Det 7, 24WS

DTIC  
ELECTE  
FEB 12 1991  
S B D

DECEMBER 1990

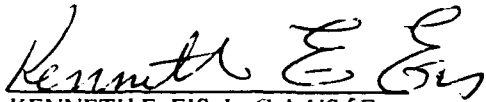
APPROVED FOR PUBLIC RELEASE;  
DISTRIBUTION IS UNLIMITED

AIR WEATHER SERVICE (MAC)  
Scott Air Force Base, Illinois, 62225-5008

91 2 11 190

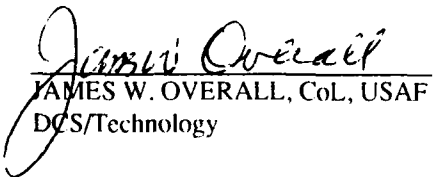
## REVIEW AND APPROVAL STATEMENT

AWS/TR-90/001, *Convective-Scale Dynamics*, December 1990, has been reviewed and is approved for public release. There is no objection to unlimited distribution of this document to the public at large, or by the Defense Technical Information Center (DTIC) to the National Technical Information Service (NTIS).



KENNETH E. EIS, Lt Col, USAF  
Directorate of Aerospace Development

FOR THE COMMANDER



JAMES W. OVERALL, Col, USAF  
DCS/Technology

## REPORT DOCUMENTATION PAGE

2. Report Date: December 1990
3. Report Type: technical report
4. Title: Convective-Scale Dynamics
6. Author: Capt Jeffrey R. Hedges
7. Performing Organization Name and Address: HQ Air Weather Service (AWS/DOTM), Scott AFB, IL 62225-5008
8. Performing Organization Report Number: AWS/TR-90/001
12. Distribution/Availability Statement: Approved for public release; distribution is unlimited.
13. Abstract: A simplified discussion of the convective process, the thunderstorm, and severe weather. Includes explanations of stability and the parcel theory. Describes thunderstorms, from "garden variety" to supercell. Tells how to recognize and forecast severe weather. Abbreviates and summarizes Doswell (1982 and 1985).
14. Subject Terms: METEOROLOGY, WEATHER, WEATHER FORECASTING, WEATHER WARNINGS, SEVERE WEATHER, CONVECTION, THUNDERSTORM, TORNADO, SQUALL LINE, DOWNBURST
15. Number of Pages: 41
17. Security Classification of Report: Unclassified
18. Security Classification of this Page: Unclassified
19. Security Classification of Abstract: Unclassified
20. Limitation of Abstract: UL

## PREFACE

After more than 15 years of studying and observing the severe storm warning process, I saw a definite need to improve the overall understanding of thunderstorms and related phenomena. Through real-time experience in the Severe Weather Unit of the Air Force Global Weather Central, I was able to learn many "snap decision" techniques for issuing severe weather warnings. As my knowledge of severe storm structure and behavior increased, so did my ability to pinpoint severe weather events before they occurred. A real test came in 1985 when I developed course curriculum in the Weather Technician Course at Chanute AFB to teach this concept to new forecasters. The information already existed, but in a format that was not very "user-friendly." It was my job to put it in a format that would be more practical and easier to understand. The result is an attempt to provide the required knowledge to all operational forecasters who have a severe weather warning responsibility.

I wish to express sincere thanks to Colonel Randolph W. Ashby and Major Steven R. Gilbert formerly of the 30th Weather Squadron, and to Major Craig R. Wikes of the Training Materials & Programs Division of Air Weather Service, for their critical reviews of this paper.

# CONTENTS

	<i>Page</i>
<b>INTRODUCTION</b> .....	1
<b>CONVECTIVE THEORY</b>	
2.1 The Three Essentials for Convection .....	2
2.2 Stability .....	2
2.3 Effects of Low-Level Moisture on Parcel Stability .....	4
2.4 Winter Convection .....	6
<b>THE THUNDERSTORM</b>	
3.1 Evolutionary Stages .....	8
3.2 Air Mass Thunderstorms .....	11
3.3 Frontal Thunderstorms .....	12
3.4 Orographic Thunderstorms .....	15
<b>THE SEVERE THUNDERSTORM</b>	
4.1 General .....	16
4.2 Multicell Severe Thunderstorms .....	16
4.3 Supercell Thunderstorms .....	20
4.4 Squall Lines .....	27
4.5 Pulse-Severe Thunderstorms .....	28
4.6 Downbursts .....	29
<b>SUMMARY</b> .....	31
<b>BIBLIOGRAPHY</b> .....	32



<b>Accession For</b>	
NTIS GRA&I	<input checked="" type="checkbox"/>
DTIC TAB	<input type="checkbox"/>
Unannounced	<input type="checkbox"/>
Justification _____	
By _____	
Distribution/ _____	
<b>Availability Codes</b>	
Dist	Avail and/or Special
A-1	

## FIGURES

	<i>Page</i>
Figure 2.1 Thermodynamic Variables on the Skew-T, Log P Diagram (from AWS/TR-79/006).....	2
Figure 2.2 Environmental (Sounding) Lapse Rate <u>Greater Than</u> Lapse Rates of Dry and Moist Adiabats (from AWS/TR-79/006).....	3
Figure 2.3 Environmental (Sounding) Lapse Rate <u>Less Than</u> Lapse Rates of Dry and Moist Adiabats (from AWS/TR-79/006).....	3
Figure 2.4 The Positive Energy Area .....	3
Figure 2.5 Convective Variables in a "Dry" Vs. "Moist" Air Mass.....	4
Figure 2.6 Environmental (Sounding) Lapse Rate Less Than Lapse Rate of Dry Adiabats, but Greater than Lapse Rate of Moist Adiabats (from AWS/TR-79/006) .....	5
Figure 2.7 Theoretical Vs. Actual Parcel Ascent .....	6
Figure 2.8 A Wintertime Mid-latitude Sounding .....	7
Figure 3.1 The Cumulus Stage of Thunderstorm Development.....	8
Figure 3.2 The Mature Stage of the Thunderstorm .....	8
Figure 3.3 Relationship Between Cloud-to-Ground Lightning and Radar Reflectivity (Log Z) .....	9
Figure 3.4 Thunderstorm Outflow and the Formation of the Gust Front.....	10
Figure 3.5 The Dissipating Stage of the Thunderstorm .....	11
Figure 3.6 The Remains of a Decayed Thunderstorm.....	11
Figure 3.7 Gust Front Diagram .....	13
Figure 3.8 Formation of a New Squall Line.....	13
Figure 3.9 An Overrunning Cold Front.....	14
Figure 3.10 Low-Level Jet Forces Unstable Air into the Warm Frontal Zone .....	14
Figure 3.11 Thunderstorm Formed Over Mountains .....	15
Figure 3.12 Synoptic-Scale Easterly Flow into the Rockies Results in Significant Orographic Lift .....	15
Figure 3.13 Differential Heating on Mountain Tops Results in Valley Breezes Converging at the Peaks .....	15
Figure 4.1 Strong Winds Aloft Carry Precipitation Downstream .....	16
Figure 4.2 Bubble of Outflow Air Blocks Inflow from Front of Storm.....	17
Figure 4.3a A Multicellular Thunderstorm Complex .....	17
Figure 4.3b A Multicellular Thunderstorm Complex Plus 10 Minutes .....	18
Figure 4.3c A Multicellular Thunderstorm Complex Plus 20 Minutes .....	18
Figure 4.4 Precipitation Distribution in a Multicellular Thunderstorm .....	19
Figure 4.5 Radar View of New Cell Regeneration in a Multicell Complex .....	19
Figure 4.6a Horizontal (PPI) Radar View of a Supercell.....	20
Figure 4.6b Vertical (RHI) Radar View of a Supercell.....	21
Figure 4.7 Three-Dimensional Representation of the Right Flank Outflow Boundary (Gust Front) .....	21
Figure 4.8 Rotating Updraft in Right Rear Flank Deforms Low-Level Radar Echo into Pendant Shape .....	22
Figure 4.9 Vertical Cross-Section of an Adult Supercell.....	22
Figure 4.10 A Supercell Deviates to the Right of Mean Upper-Level Flow .....	23
Figure 4.11a Three-Dimensional Airflow Schematic in a Supercell--Initiation of RFD.....	23
Figure 4.11b Three-Dimensional Airflow Schematic in a Supercell--RFD Reaches the Surface .....	24
Figure 4.11c Three-Dimensional Airflow Schematic in a Supercell--The RFD Strengthens.....	24
Figure 4.11d Low-Level Airflow Schematic in a Tornado-Producing Supercell .....	25
Figure 4.11e Three-Dimensional Airflow Schematic in a Supercell--the Updraft Collapses.....	26
Figure 4.12 Look-Down View of a Tornadoic Thunderstorm, Showing Observed Features .....	26
Figure 4.13a Vertical (Look-Down) View of Squall Line .....	27
Figure 4.13b Cross-Sectional (Side) View of Squall Line.....	28
Figure 4.14 Radar Depiction: Evolution of an Ordinary Thunderstorm (top), and a Pulse Storm (bottom) .....	29
Figure 4.15 Radar Depiction: The Life of a Bow Echo on 6 August 1977.....	30

## INTRODUCTION

Severe convective storms are predictable. They have been routinely forecast with increasing accuracy since the late 1940s. When these storms threaten, people are still frightened. But because they are generally warned, more survive, with fewer injuries. Since fatalities obviously still happen, and since people still rush to cover because of "false alarms," we still have a long way to go in improving severe storm prediction.

Increasing numbers of less experienced forecasters are being given the awesome responsibility of protecting lives and property from the devastating effects of severe convective weather. Even though technology has advanced tremendously, it cannot completely substitute for a lack of forecasting experience. Too many warnings are issued for severe convective phenomena that never appear. Too many decisions are made solely on the basis of visual sightings relayed to the forecaster, or by basic pattern and shape recognition such as a radar signature. Too often, not enough thought is given to the structure and behavior of severe convective storms before making critical decisions that send people to their cellars. The results are unreliable warnings and loss of faith in the forecaster.

To help reduce the number of warnings issued blindly, the author developed an instructional program at the

Chanute AFB Technical Training Center that teaches forecaster students the dynamics of convective storms. Step-by-step, students are taken from basic parcel stability, through basic convection, and finally, to the structure of severe convective storms. With this building block approach, students learn how and why convective storms develop and produce destructive phenomena. When confronted with forecasting and warning situations, these students are better prepared for convective activity; decisions are based on logic rather than on panic and reflex.

This report is intended to provide readers with a similar foundation in convective scale dynamics. It is far from comprehensive, but if the forecaster reads, understands, and applies its contents, the result should be improved ability to handle severe weather situations with confidence. As we enter the era of Doppler radar, it becomes even more important to have a thorough understanding of the structure and behavior of convective storms. Doppler radar will provide forecasters with a far more complex look at the thunderstorms than ever before. The three-dimensional views, vortex signatures, and velocity gradients will produce imagery that can be used by knowledgeable operators to give their customers what they need: timely and accurate severe weather warnings, with fewer false alarms.

## CONVECTIVE THEORY

**2.1 The Three Essentials for Convection.** No matter whether we deal with ordinary convective showers or severe tornado-producing thunderstorms, three ingredients must be present in one form or another; the ability to recognize them is the basis for forecasting convective activity:

- a convectively unstable atmosphere
- a low-level moisture source for fuel
- a triggering mechanism

**2.2 Stability.** The evolution of deep convection and thunderstorms has its basis in the parcel theory, a simple expression of density differential which states that if a parcel of air is *warmer* than its surroundings, it will rise; under these conditions, the atmosphere is *unstable*. If the parcel is *cooler* than its environment, it will sink; under these conditions, the atmosphere is *stable*. For simplicity, the parcel theory assumes that no exchange of heat or moisture takes place between the parcel and its environment. The most practical way to illustrate the parcel theory is to use a Skew T, Log P diagram, a simplified version of which is shown in Figure 2.1.

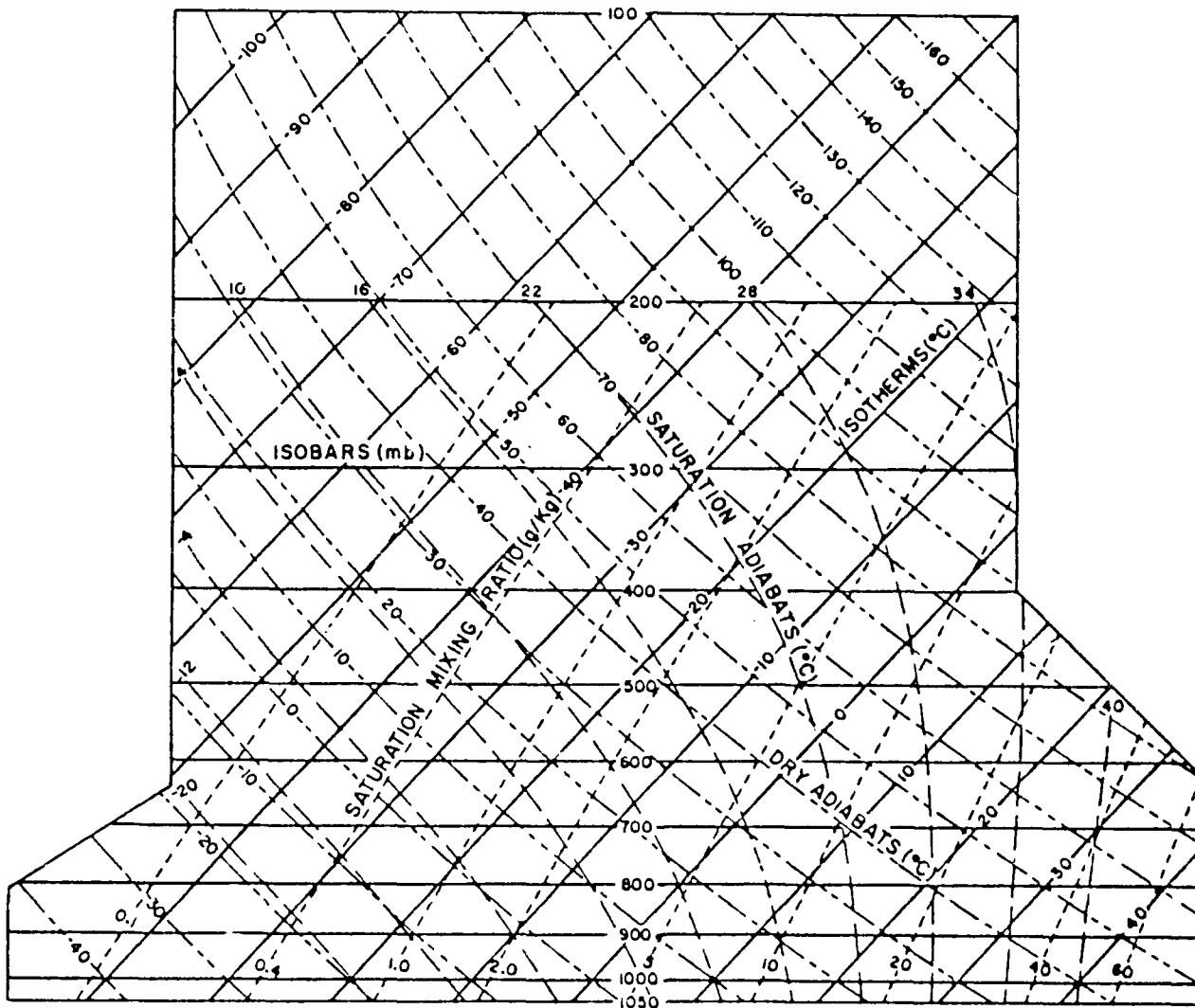


Figure 2.1 Thermodynamic Variables on the Skew T, Log P Diagram (from AWS/TR-79/006). Note how the slopes of the dry and pseudo-adiabats (also called "saturation" or "moist" adiabats) vary with temperature. Note also how temperature affects the saturation mixing ratio.



A lifted parcel of air expands as pressure decreases. For an unsaturated parcel, the expansion results in cooling the parcel by about  $10^{\circ}\text{C}/\text{Km}$ . This is known as the "dry adiabatic lapse rate" ( $\Gamma_d$ ), and is represented by the dry adiabats on the Skew T diagram. Note that  $\Gamma_d$  remains fairly constant from high to low temperatures in the lower atmosphere. For a parcel to remain buoyant and ascend freely, the environmental lapse rate ( $\Gamma_e$ ) must be greater (that is, less vertical) than  $\Gamma_d$ . In this situation (which is seldom found in the real world), the atmosphere is considered to be *absolutely unstable*, as shown in Figure 2.2. Once a parcel has achieved buoyancy, it will continue to rise as long as it remains warmer than its environment. This usually continues up to the tropopause, where the environmental lapse rate becomes isothermal.

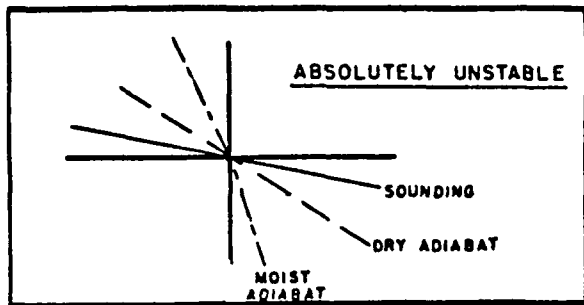


Figure 2.2 Environmental (Sounding) Lapse Rate Greater Than Lapse Rates of Dry and Moist Adiabats (from AWS/TR-79/006).

Once the parcel temperature equals environmental temperature, equilibrium is achieved. Except for some overshooting due to momentum, the ascent ceases, and the mass that overshoots will eventually return to the equilibrium level (EL). The parcel, unless subjected to lifting forces, cannot progress into the warmer air above the EL because it would be colder (and therefore denser) than its environment. The region above the EL would be considered *stable*--see Figure 2.3. The EL is where convective clouds generally flatten out and become anvil-shaped. When momentum carries a parcel above the EL, a cumuliform dome (or "overshooting top") extends above the anvil deck.

That region of the atmosphere in which the air parcel is warmer and more buoyant than its environment is called a "positive energy area" and is shown in Figure 2.4. The greater the temperature difference between the

parcel and its environment ( $T_p - T_e$ ), the greater the positive energy area and the faster the ascent. Rising parcels are referred to as "updrafts."

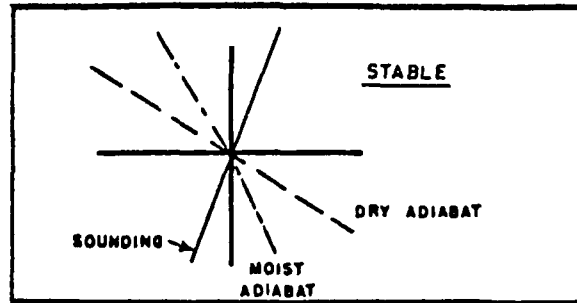


Figure 2.3 Environmental (Sounding) Lapse Rate Less Than Lapse Rates of Dry and Moist Adiabats (from AWS/TR-79/006).

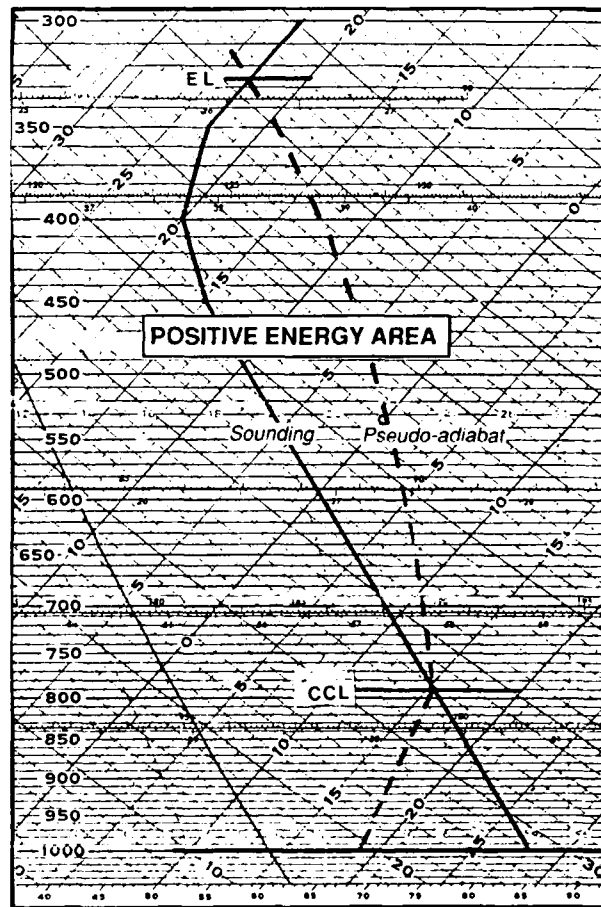


Figure 2.4 The Positive Energy Area. A buoyant air parcel inside the positive energy area rises from the convective condensation level (CCL) until it reaches equilibrium with its environment at the equilibrium level, or EL.

**2.3 Effects of Low-Level Moisture on Parcel Stability.** Atmospheric moisture contains a substantial amount of latent heat energy. When released, this energy has a pronounced effect on parcel buoyancy. As moisture content increases, so does the amount of latent heat available for release. The temperature of the air mass has a direct effect on its ability to hold moisture. This can be seen (in Figure 2.1) by comparing the saturation mixing ratios (at a constant pressure) for warm and cold air. At 1,000 mb, air at 10°C can hold a maximum of 8g/Kg, while air at 30°C can hold a maximum of 29g/Kg.

When an unsaturated parcel of air containing moisture ascends, its temperature decreases dry adiabatically until it reaches saturation. If the parcel rises because of forced lift, saturation occurs at the *lifting condensation level*, or LCL. If the parcel rises because of heating from below, saturation occurs at the *convective condensation level*, or CCL. The LCL for a surface parcel is always located at

or below the CCL. Once saturation occurs, either at the LCL or CCL, the additional sensible heat given off by the condensation process (latent heat) slows the cooling rate of the rising parcel. This new cooling rate establishes a new *pseudo-adiabatic* lapse rate,  $\Gamma_c$ .

As already mentioned, when the atmosphere's moisture content increases, so does the amount of latent heat available for release. Note (in Figure 2.1) that at higher temperatures, the slopes of the pseudo-adiabats are much steeper than those of the dry adiabats ( $\Gamma_c \ll \Gamma_d$ ), the direct result of the large amount of latent heat released during condensation. At lower temperatures, much less latent heat is available due to the low moisture content, and the slopes of the pseudo-adiabats and dry adiabats become nearly parallel. This relationship contributes to the seasonality of thunderstorms, which will be discussed later. The effects of moisture content on parcel stability are shown in Figure 2.5.

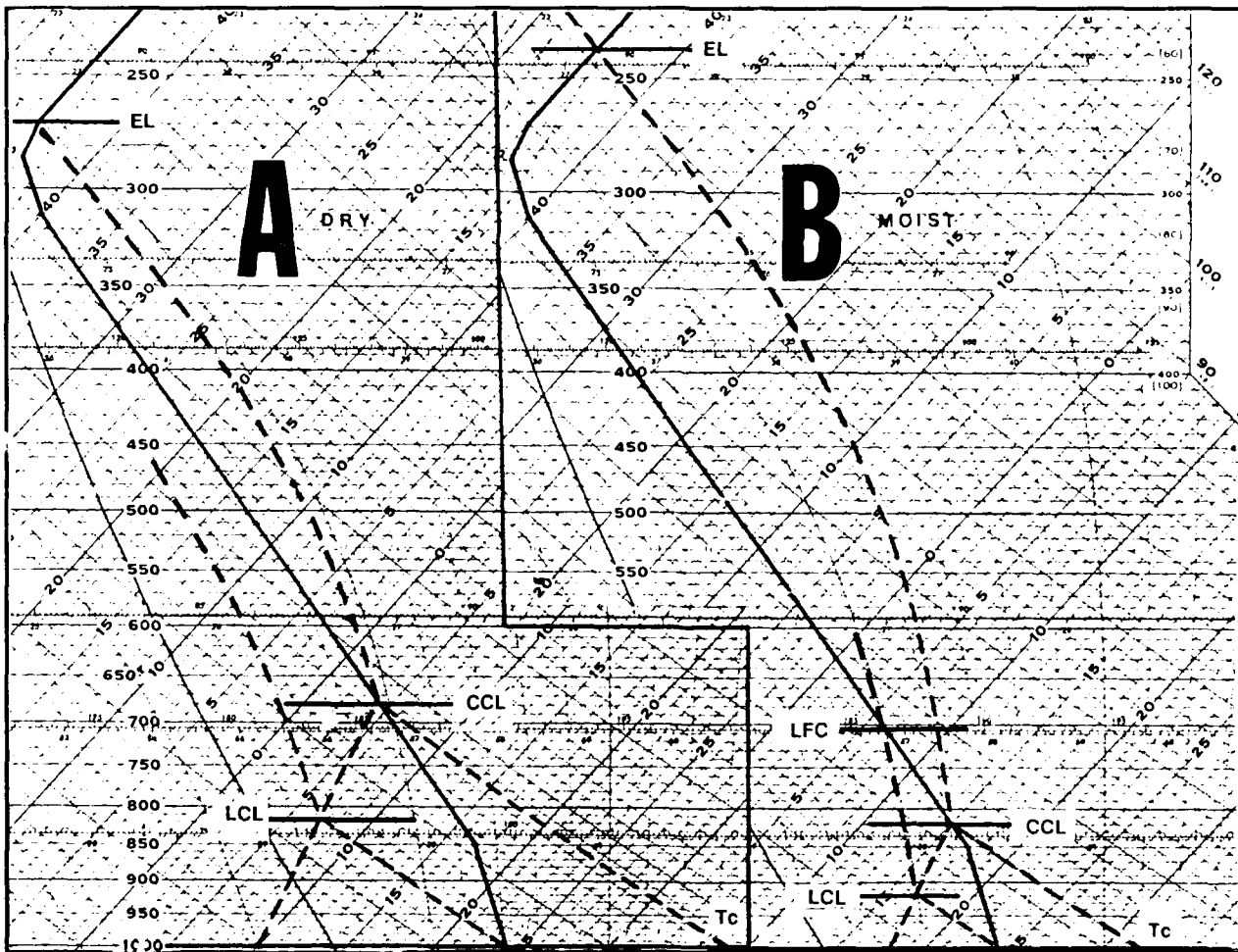


**Figure 2.5 Convective Variables in a Dry Vs. Moist Air Mass.** "A" is a sounding in a dry air mass. "B" is the same vertical profile, but with increased low-level moisture. Convective temperature is shown as  $T_c$ .

First, consider the dry sounding profile on the left (A) side of Figure 2.5. If the surface air mass has a dewpoint of 50°F (10°C), the CCL will be at 683 mb. To reach condensation by surface heating alone, the surface (or convective) temperature ( $T_c$ ) would have to be 98°F (37°C). Note the weak positive energy area from the CCL to the EL at 270 mb. If low-level moisture content were to increase, substantial changes would take place, as shown on the right (B) side.

The "B" side of Figure 2.5 shows the same vertical profile as "A," but with a surface dewpoint of 65°F (18°C). Because of the higher moisture content, the CCL (at 820 mb) is much lower. Besides producing lower cloud bases, the lower CCL allows convective cloud formation with a much lower surface temperature (in this case, 89°F/32°C), and greatly increases the probability of convection.

In the moist case (side "B"), the positive energy area becomes enormous compared to the "A" side: in fact, the parcel-to-environment temperature difference at 300 mb is nearly three times larger! Parcels are far more buoyant and ascend more rapidly. Updraft speeds are much greater, and the EL much higher. Convective clouds build to greater vertical extents. With higher updraft speeds and momentum, parcels overshoot the EL far more than in the drier case shown in the "A" example where, if upward motion were to be achieved by mechanical lifting, the LCL would be at 810 mb.

Parcel buoyancy is never reached in what would be considered a "negative energy area," where the atmosphere is *stable*. But with the increased low-level moisture shown in "B," parcel buoyancy is achieved at 720 mb--the *level of free convection* (LFC). Under these conditions, the atmosphere is *unstable*; hence, the concept of *conditional instability* ( $\Gamma_c < \Gamma_e < \Gamma_d$ )--see Figure 2.6.

If the environmental lapse rate falls off even more slowly with height than the pseudo-adiabatic lapse rate, or even if it *increases* with height as in an inversion, the parcel could not achieve buoyancy under any condition. This condition is referred to as being *absolutely stable* ( $\Gamma_e < \Gamma_c$ ).

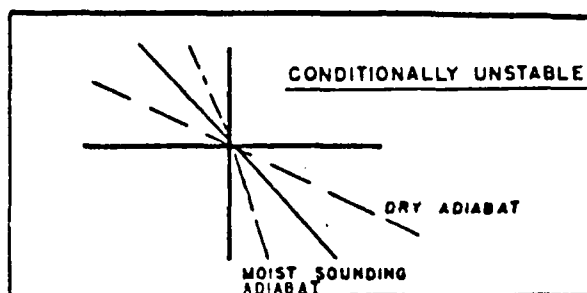


Figure 2.6 Environmental (Sounding) Lapse Rate Less Than Lapse Rate of Dry Adiabats, but Greater than Lapse Rate of Moist Adiabats (from AWS/TR-79/006).

The real atmosphere, however, seldom behaves according to parcel theory. Not every cumulus cloud becomes a thunderstorm, even though its vertical profile may be conditionally unstable to great heights. Parcels actually undergo heat exchange and mix with drier environmental air through a process known as *entrainment*. This effect, greatest at the periphery of clouds, results in evaporation that causes parcels to cool at a faster rate than that suggested by parcel theory.

Figure 2.7 shows the difference between parcel theory and reality. The most obvious feature in the example is the lower cloud top, the result of the early attainment of equilibrium common with small parcels. This is observationally sound: cumulus and towering cumulus predominate on thunderstorm days.

Most studies, however, show that cumulus actually consists of variously developed and evolving larger parcels, or "buoyant plumes." These plumes are variously exposed to and penetrated by entraining environmental air. The inner plumes, or cloud cores, are more protected from entrainment. As they continually push to greater and greater heights, they condition the air above with warmer and moister air. This eventually allows the core plumes to rise high enough to produce a thunderstorm. The answer to what determines whether or not a thunderstorm will develop, however, is not a simple process, but some possibilities will be examined later.

For a more complete discussion of atmospheric instability, see AWS/TR79/006 (Revised).

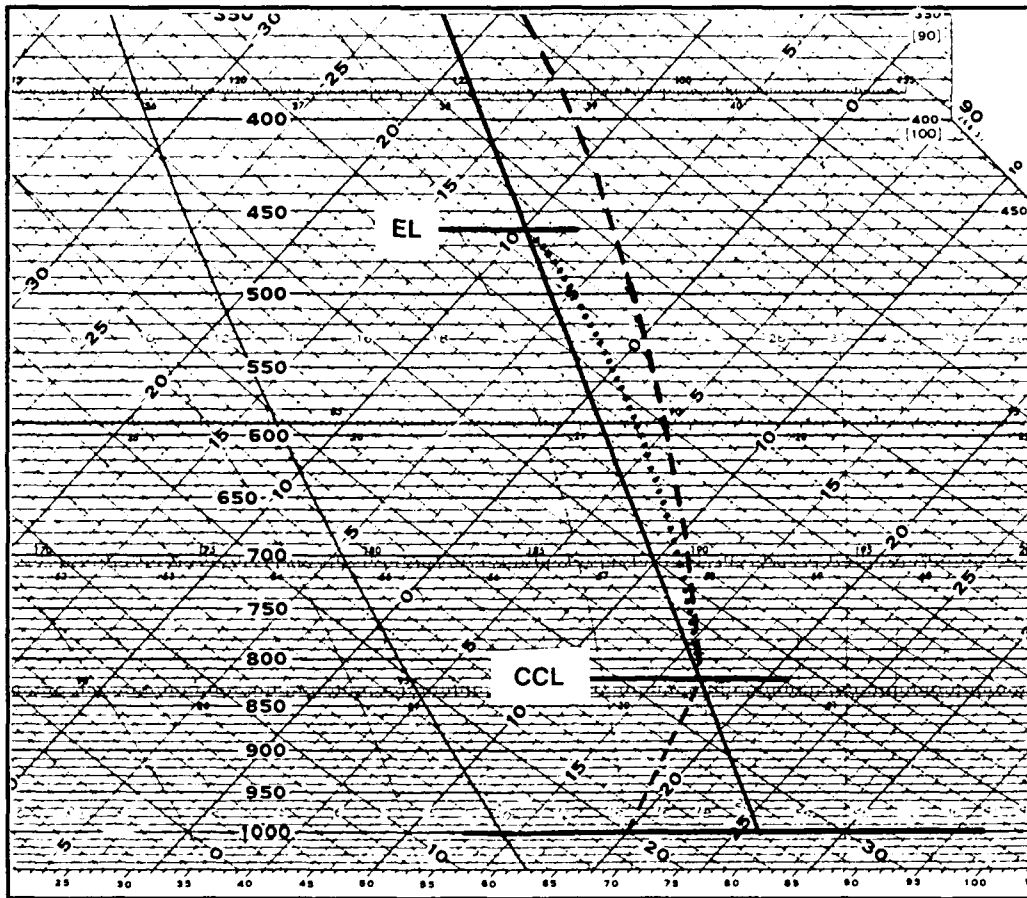


**Figure 2.7 Theoretical Vs. Actual Parcel Ascent.** The dashed line represents the parcel theory ascent, while the dotted line represents the actual case. A small parcel loses heat to the environment during its ascent. The result is a larger  $\Gamma_s$  and a lower EL.

**2.4 Winter Convection.** Thunderstorms are much less frequent in cold than in warm seasons. This is easy to understand when we apply the convective principles just discussed. Even at saturation, cold polar air masses cannot hold much moisture. This limits the amount of latent heat available for release into a rising parcel, and only a small reduction in the cooling rate results. The result is a pseudo-adiabatic lapse rate only slightly less than the dry adiabatic rate.

But winter thunderstorms *do* occur, and probably more often than many meteorologists realize. The key to wintertime thunderstorm formation is penetration of the  $-20^{\circ}\text{C}$  isotherm aloft. Empirical evidence, supported by recent research, indicates that convection must exceed this level to create an electrical charge strong enough to produce lightning.

Three synoptic conditions favor winter thunderstorms; they are: (1) strong dynamic weather systems with an active warm sector that contains maritime tropical (mT) air; (2) very cold air passing over much warmer water such as the Great Lakes of North America, and (3) deep, very intense cold-core cyclones.

Strong dynamic systems that pull mT air into the warm sector of a cyclone overrunning the warm front are excellent wintertime thunderstorm generators. Although the mT air is sufficiently unstable, it is usually aloft and not evident at the surface, which is still cold. As a result, thunderstorms are usually confined to the region just north of the warm frontal boundary. If the thunderstorm precipitation is snow, very large accumulations can occur in a short period of time.

Very cold air passing over warm water produces strong and extensive convection that can develop into thunderstorms. Even though the invading air mass itself is stable, the lowest layer becomes unstable when heated through contact with the warm water. Near-superadiabatic lapse rates are produced by the combination of warm moist surface air and the bitterly cold air above it. The result is shallow (usually less than 10,000 feet deep) but vigorous convection. Heavy snowshowers frequently result, but lightning is rare. Electrical discharges have been triggered, however, when aircraft penetrate convective clouds. This type of activity is common along the lee shores of the Great Lakes, where it is referred to as a "lake-effect snowshower." These showers are the primary cause of the Great Lakes lee side "snow belts."

The third condition that favors the formation of winter thunderstorms is the slow-moving, intense, well-developed upper-level cyclone. Such systems always

have a deep pool of very cold air surrounding the center and extending to the tropopause. These systems, normally behind the surface front, are capable of producing diurnal thunderstorms, occasionally accompanied by small hail, damaging winds, and even cold air tornadoes. Such systems are normally found over and along the western coasts of temperate zones--notably the United States and Europe--but they can occur inland, as well. Convection can be surprisingly deep--sometimes exceeding 30,000 feet MSL.

Figure 2.8 is an example of a wintertime, mid-latitude sounding profile. Mid-latitude winter is characterized by brief solar days with low angles of insolation, resulting in far less surface heating than in summer. When combined with the high albedo of snow cover, it is highly unlikely that surface heating can produce enough thermal lift to reach condensation ( $T_c$ ). Therefore, some form of mechanical lift or other strong dynamic influence is required to produce convection.

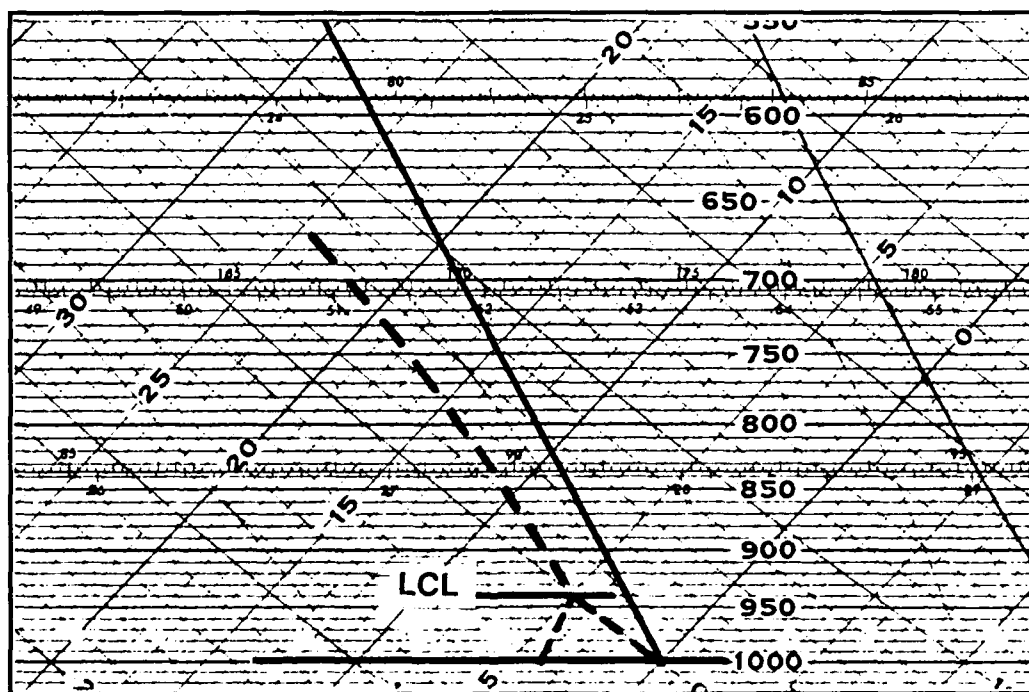


**Figure 2.8 A Wintertime Mid-latitude Sounding.** The lack of moisture in a winter air mass limits the amount of latent heat available for release and effectively prevents a parcel from achieving buoyancy. The parcel temperature remains cooler than the environment through its entire ascent. It will never achieve buoyancy even though the low-level air mass is relatively moist. Mechanical (frontal, orographic) or dynamic (upper-level divergence) lifting processes are the only means left to provide the needed upward motion. The vertical speeds here are usually much less and occur over a much wider area than convective updrafts, resulting in lighter and more uniform precipitation.

# THE THUNDERSTORM

**3.1 Evolutionary Stages.** With a basic understanding of parcel stability, we can now discuss the evolution of the most dramatic convective event--the thunderstorm. Early researchers (Byers and Braham, 1949) laid the foundation for the study of thunderstorm structure and development by classifying them into three different categories, or stages of evolution: these are the *cumulus*, *mature*, and *dissipating* stages. Each is shown and discussed below.

The *cumulus* stage shown in Figure 3.1 is marked by the formation of the first convective cloud. With its base at or slightly above the CCL, the cloud is dominated by the updraft as it grows toward its equilibrium level. As more and more low-level moisture is pumped into the growing cumulus, relatively large liquid hydrometeors begin to form in its upper regions. (The term *hydrometeor* is used to describe any product of condensation or sublimation of atmospheric water vapor (liquid or solid) that may or may not fall out as precipitation.)

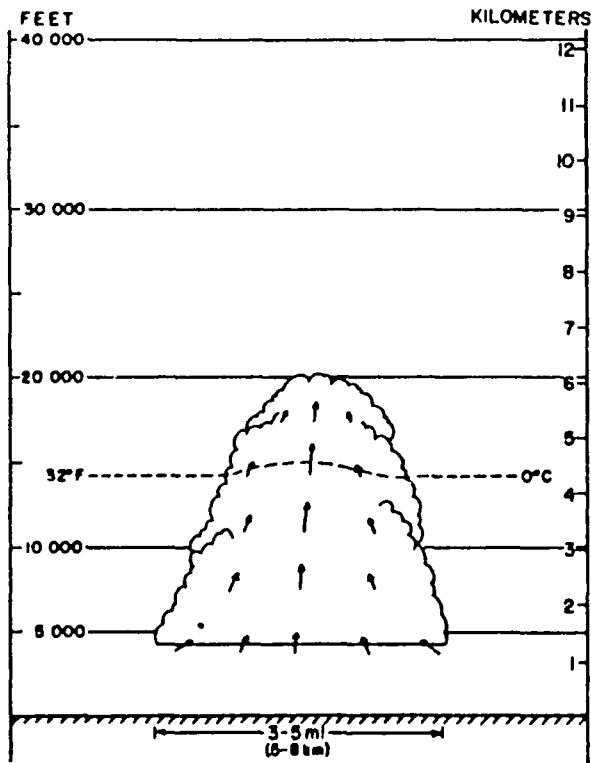


**Figure 3.1** The Cumulus Stage of Thunderstorm Development. Updrafts prevail as large hydrometeors form in the upper portions of the cloud (Doswell, 1985).

From the outside, the cloud top may seem to lose definition as the cloud droplets turn to ice crystals. This process (glaciation) appears to correlate well with the formation of precipitation. A radar echo aloft should now begin to appear. The updraft continues to hold the prospective precipitation aloft until it accumulates beyond the point at which its weight can be supported. It then falls against the updraft and begins to create a downdraft due to frictional drag. When the precipitation reaches the surface, the second, or *mature*, stage has begun.

The mature stage is the most active and violent. As shown in Figure 3.2, updrafts and downdrafts coexist in the same cell. The cloud reaches its maximum vertical extent, flattening out into the familiar anvil at the equilibrium level. Carried by the winds at that level, the anvil usually elongates downstream. Although heavy precipitation is common, it may not reach the surface in extremely arid regions.

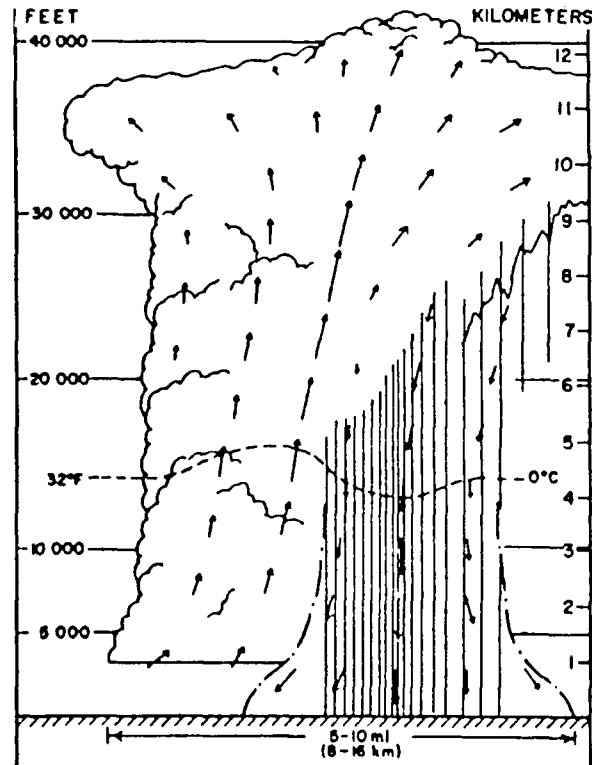


**Figure 3.2** The Mature Stage of the Thunderstorm. Falling hydrometeors create the downdraft. Tops reach the EL and assume the anvil shape. (Doswell, 1985).

An apparent by-product of the precipitation process is thunder and lightning. There seems to be a direct correlation between lightning frequency and rainfall rate. Figure 3.3 shows this relationship, using radar reflectivity to represent rainfall rate.

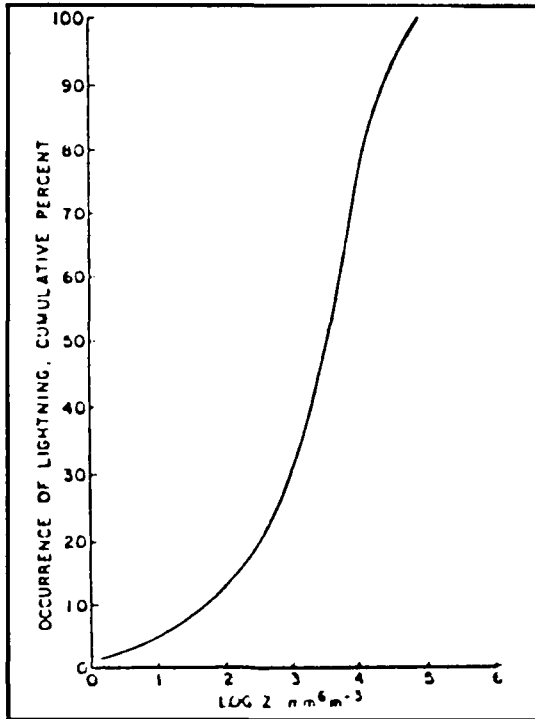


**Figure 3.3 Relationship Between Cloud-to-Ground Lightning and Radar Reflectivity (Log Z).** The occurrence of cloud-to-ground lightning increases with rainfall rate (From Kinzer, 1972).

As mentioned earlier, *precipitation drag* is the primary downdraft mechanism. Although it would seem

that the heavier the precipitation, the stronger the downdraft, this is not always so. In arid regions, violent downdrafts from clouds with high bases are common, but there is very little precipitation at the surface. An important factor here is the presence of dry air in the thunderstorm environment. If dry air enters the convective cloud (generally by entrainment), evaporation of cloud droplets takes place, with a corresponding drop in temperature. This increases the density of the air and gives it a tendency to sink. This process is thought to be a significant downdraft enhancement mechanism in nearly all thunderstorms. It requires a delicate balance, because too much dry air would completely evaporate the cloud.

Another effect of dry air entrainment is the destabilization of the immediate cloud environment from evaporative cooling at the cloud's edge. When this occurs in the storm's mid-levels, the rising parcels sense a cooler surrounding environment and ascend faster. Pioneer severe weather forecasters (Fawbush, et al., 1951) recognized the importance of dry air to the severe storm, and incorporated the analysis of dry air regions into severe weather forecasting routines. It is still widely used today.

When the downdraft reaches the surface, it spreads out horizontally as a new air mass--see Figure 3.4. The leading edge of this outflowing air is known as the "gust front," or "outflow boundary." Surface winds shift drastically with the passage of a gust front; they can attain damaging speeds, depending on the strength of the downdraft. Aircraft are particularly vulnerable to these windshifts. Headwinds change into crosswinds or tailwinds in seconds to produce the deadly phenomenon known as "low-level wind shear." But people on the ground often welcome a gust front as the fresh and cool pre-thunderstorm breeze that replaces warm and muggy tropical air.

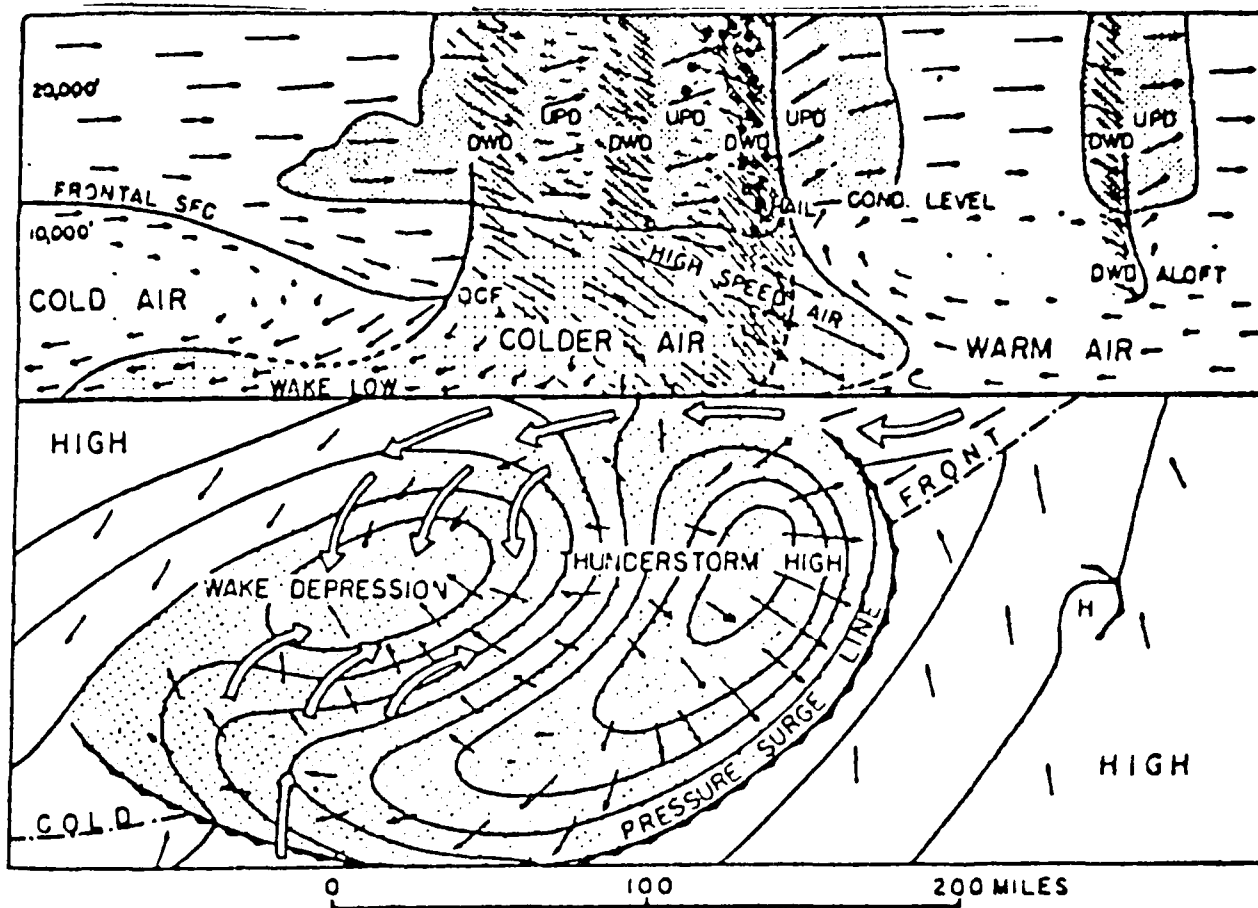


Figure 3.4 Thunderstorm Outflow and the Formation of the Gust Front (Fujita, 1955).  
Downdrafts are identified by "DWD," updrafts by "UPD."

The updraft continues to hold hydrometeors aloft. Ice crystals suspended near the melting level alternate between freezing and melting, accumulating a water coating as they move up and down in and around the updraft core. The result is a hailstone, which continues to grow until it is too heavy to be supported by the updraft. The stronger the updraft, the larger the hailstone. Once a hailstone falls below the freezing level, it begins to melt. It continues to melt until it reaches the surface, unless it melts completely first. The height of the melting/freezing level is near the  $0^{\circ}$  isotherm; the height of the wet-bulb zero, therefore, is significant in determining the size of a hailstone at the surface. Miller (1972) reported that a wet-bulb freezing level (wet-bulb zero) of 7,000-9,000 feet AGL is the optimum height for producing large hail at the surface. Although a lower wet-bulb freezing level may be favorable for hailstone survival, it may not be favorable for thunderstorm development because the air mass

would be too cold. In tropical regions, where the wet-bulb-zero is relatively high, surface hail reports are rare. For aviation, it's important to remember that hail can, and probably will, be encountered aloft even when it is not observed at the surface.

Another product of updraft-downdraft interaction is turbulence. Many aircraft have been destroyed during attempts to penetrate thunderstorms. Even small thunderstorms, as observed from the surface, are capable of severe to extreme turbulence. Expect at least severe turbulence in and near any thunderstorm cell.

The formation of the downdraft, which marked the beginning of the mature stage, also signals the *dissipating* stage, which actually begins when the updraft collapses. With gravity on its side, the downdraft soon dominates. Outflow air eventually cuts off the inflow of warm, moist air into the storm. With the moist inflow



cut off and the updraft weakened, the precipitation process begins to shut down. Without a strong updraft, large hydrometeors can no longer form, leaving only light rain or drizzle and generally light winds at the surface. Although violent electrical activity usually ceases, the cloud can retain a charge and remain a hazard to aircraft for some time.

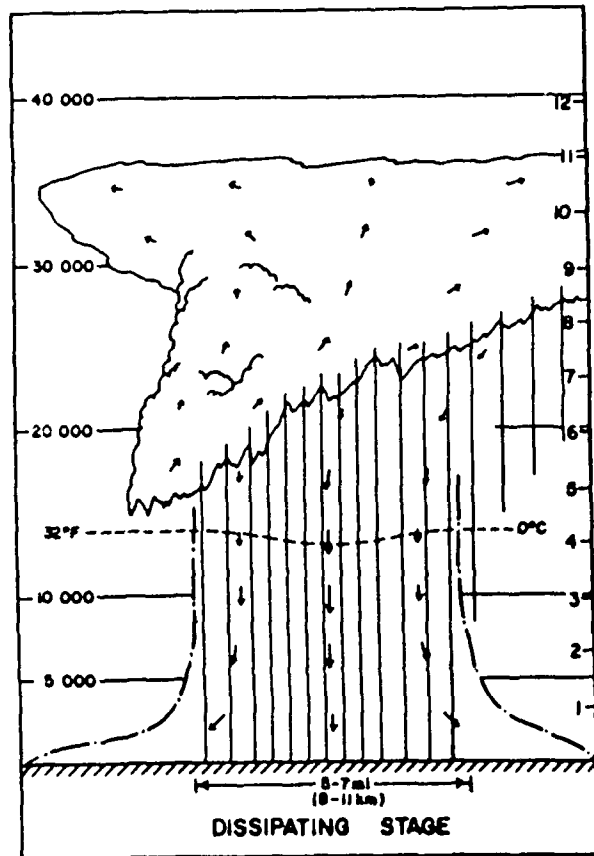


**Figure 3.5 The Dissipating Stage of the Thunderstorm.** With the updraft cut off, precipitation diminishes. Weak downdrafts prevail. (Doswell, 1985)

With subsidence prevailing, the cloud-forming process stops. The giant cumulonimbus begins to stratify into layered clouds and is eventually torn apart by the winds aloft. Eventually, all that remains is a patch of middle and high clouds that satellite meteorologists refer to as "convective debris." At the surface, a large bubble of rain-cooled outflow air is left behind. Even though it is relatively stable, this bubble can play a role in future thunderstorm development due to convergence and lifting along its boundaries. The life cycle of a typical thunderstorm cell can be completed in as little as 30 minutes.

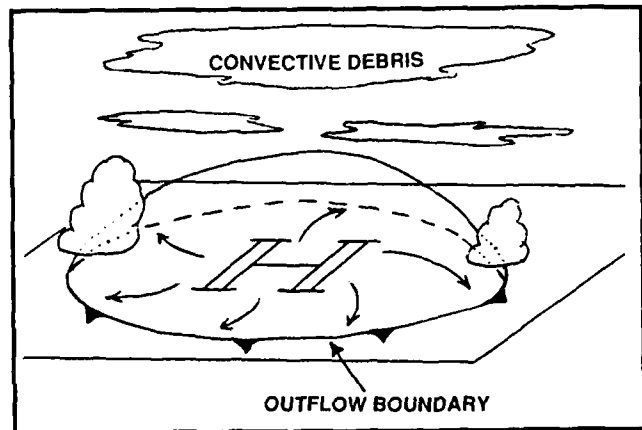


**Figure 3.6 The Remains of a Decayed Thunderstorm.** The "bubble high" of outflow air remains for some time. New convection frequently forms from the lifting along the old outflow boundary, or gust front.

**3.2 Air Mass Thunderstorms.** As the name implies, this type of thunderstorm forms within a relatively homogeneous air mass (usually mT) with little or no synoptic scale features such as fronts or upper troughs. Although it had been thought for years that air mass thunderstorms occur at random, with no apparent triggering mechanism other than surface heating, recent studies (Purdum, 1979) show that air mass thunderstorm development is actually organized and predictable. Although surface heating is an important mechanism, it appears that low-level convergence is most important in determining where deep convection will begin. Low-level convergence can result from outflow boundary interaction, terrain irregularities, or sea/lake breeze fronts, to name just a few causes.

The air mass thunderstorm fits the three-stage model just discussed very well. Its lifespan is generally less than an hour, but the regeneration of new cells often gives the impression that it lasts longer. Since surface heating is a triggering mechanism, air mass thunderstorms are almost exclusively a late afternoon phenomenon; they are rare late at night or in early morning. Air mass thunderstorms prefer deep summer when the low-level moisture content is high. Winds aloft, generally very weak, prevent cells from moving appreciable distances, and many cells remain stationary throughout their life cycle. The high moisture availability, combined with lack of movement, can result in locally heavy rainfall, common throughout the southeastern U.S.

Air mass thunderstorms rarely last long enough to develop the power required for severe weather production. Large hail, for example, requires a powerful and persistent updraft for its formation. The high freezing level common to air mass thunderstorm development also helps keep hail from reaching the ground. Damaging winds and tornadoes usually require the strong dynamic influences of jet stream winds, typically absent in air mass thunderstorm development.

**3.3 Frontal Thunderstorms.** Thunderstorms that form with synoptic-scale frontal systems are generally more violent than air mass types. The strong mechanical lifting associated with advancing fronts, especially cold fronts, provides a strong boost to updraft strength and helps sustain it over longer periods of time. As a result, frontal thunderstorms generally last longer than air mass types, averaging 1-3 hours. The presence of winds aloft above a frontal system, combined with the movement of the front itself, results in substantial movement of thunderstorm cells. Frontal thunderstorms frequently

form in bands or lines parallel to the front, as opposed to the isolated cells or clusters common to air mass thunderstorms. Frontal lifting, which undergoes little diurnal variation, allows these thunderstorms to form day or night, but they favor late afternoon and early evening due to the additional support from surface heating. It is during these late afternoon and early evening hours that severe weather events are most common.

Fast moving cold fronts usually produce the most violent thunderstorms. If these fronts move into an unstable air mass, thunderstorms may form rapidly into a squall line. A prefrontal squall line may form if conditions are favorable ahead of the front.

As the squall line builds vertically, the stronger upper-level winds influence cell movement and frequently cause the squall line to outrun the surface front. The squall line can continue to support itself by generating new cells along its advancing gust front, as shown in Figure 3.7.

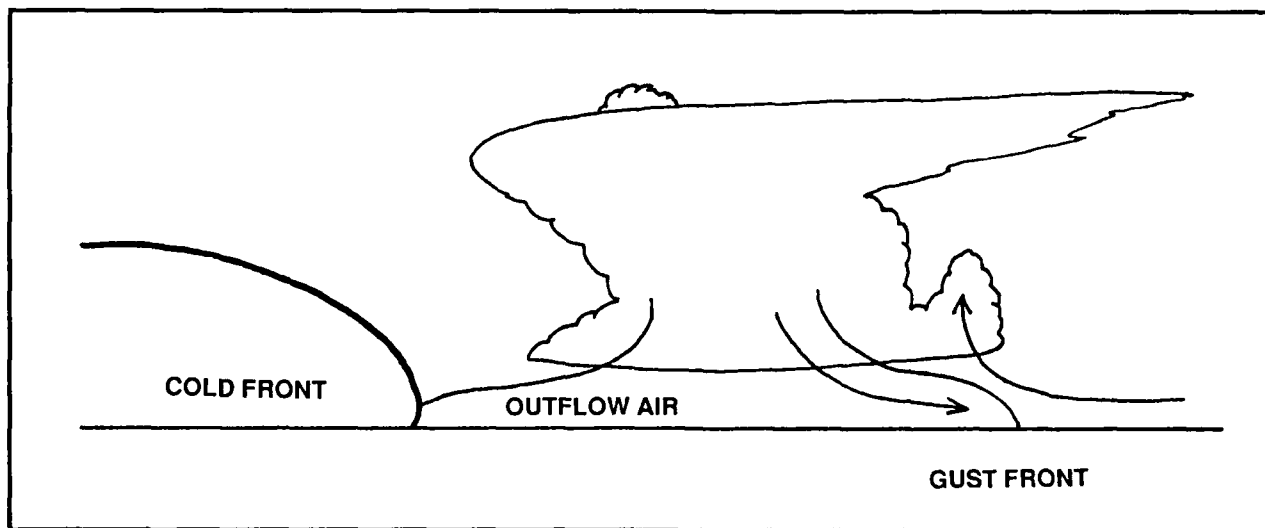


**Figure 3.7 Gust Front Diagram.** The gust front, created by the advancing outflow, provides a lifting mechanism to generate new thunderstorm activity ahead of the advancing squall line.

As the squall line moves away, a large bubble of outflow air (a mesohigh) is left in its wake, often masking the location of the actual front. This can lead forecasters to believe that frontal passage has occurred

with squall line passage. This can be a fatal mistake, because warm, moist air may creep back in behind the bubble high, with a new squall line forming as the true front again disturbs the unstable air mass (Figure 3.8).

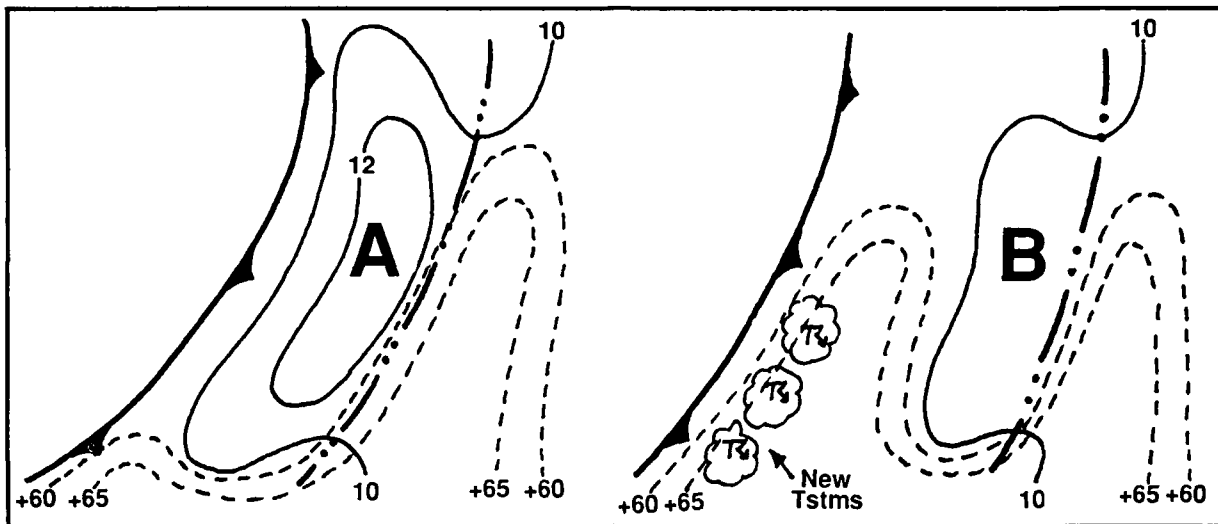


**Figure 3.8 Formation of a New Squall Line.** In "A," the squall line moves away from the front, leaving a large bubble of rain-cooled air in its wake. If, as in "B," the squall line moves far enough ahead, unstable air may creep in behind the outflow air and result in the formation of a new squall line. Isodrosotherms are dashed, isobars are solid.

Thunderstorms that form with slow-moving cold fronts are usually mild compared to those formed from fast-moving cold fronts. Since the perpendicular wind component decreases with height, the prefrontal air mass is lifted up and over the front. This results in

thunderstorm activity to the rear of the surface frontal boundary, as shown in Figure 3.9. Thunderstorms are normally embedded in stratiform precipitation, and significant downrush winds are rare. Cells move parallel to the front with the upper-level winds.

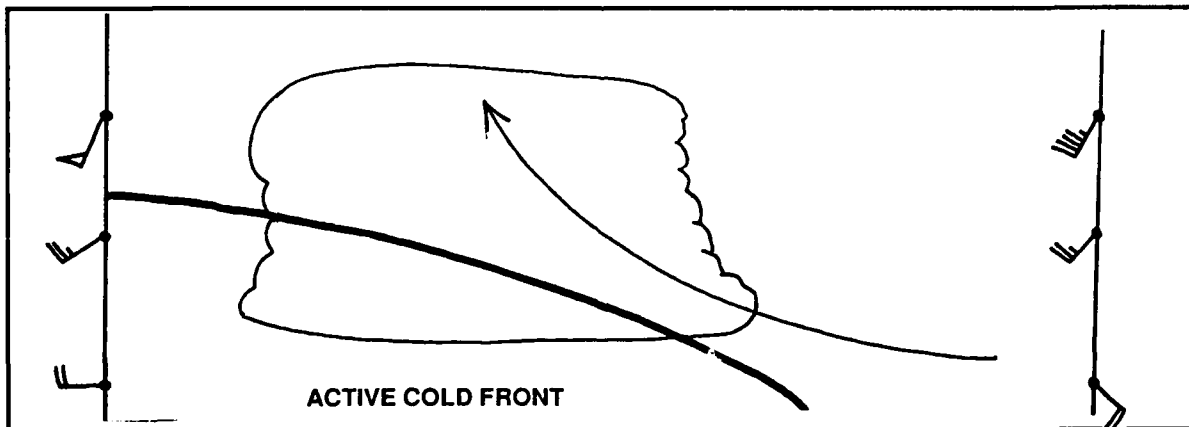


**Figure 3.9 An Overrunning Cold Front.** The overrunning nature of the slow-moving cold front produces thunderstorm activity to the rear if the air mass being lifted is unstable. Wind plots represent vertical wind profiles at the points indicated.

Warm (and stationary) frontal thunderstorms are similar to slow-moving cold frontal thunderstorms. The slope of the warm front is much shallower than that of the cold front, and lifting is very gradual. Since parcels ascend slower, their temperatures have more time to modify; buoyancy, therefore, may never be achieved, even if the overrunning air mass is unstable. This condition is favorable for stratiform precipitation. To produce thunderstorms in this situation, the unstable overrunning air usually must be forced into the warm frontal zone by strong flow, such as the low-level jet shown in Figure 3.10. In addition, the low-level jet also plays a significant role in destabilizing the warm sector due to low-level moisture and temperature advection.

Warm frontal thunderstorms are not frequent producers of severe weather. But don't confuse warm frontal thunderstorms with those that form at the intersection of another boundary and the warm front. In midsummer, warm fronts can easily trigger thunderstorm activity because the air mass is so unstable that even the slightest lifting is enough. Warm fronts are usually so weak this time of year that they occasionally escape detection.

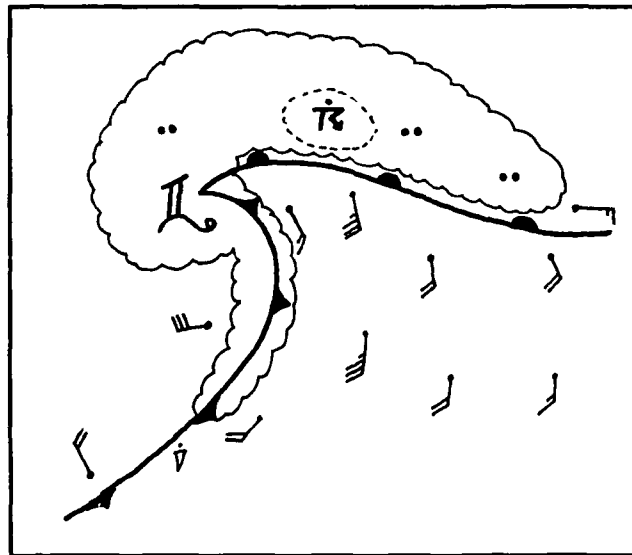


*Figure 3.10 Low-Level Jet Forces Unstable Air into the Warm Frontal Zone. Warm frontal thunderstorms are generally embedded in stratiform precipitation. Strong low-level winds help force the unstable air high enough to reach the LFC.*

**3.4 Orographic Thunderstorms.** Terrain barriers are capable of providing lift that far exceeds that of any frontal system. As an example, compare the slope of the Rocky Mountains to that of the typical cold front. Although the result of orographic lifting is usually stratiform precipitation, thunderstorms may develop in an unstable air mass. Orographic thunderstorms are particularly successful at producing very strong downrush winds, especially in the western U.S., where dry air is often available for entrainment into the storm. Terrain itself can be a significant factor, since the downrush is essentially directed downslope due to gravity--see Figure 3.11. Channelling or funnelling of downrush winds into canyons or valleys can increase wind speeds dramatically.

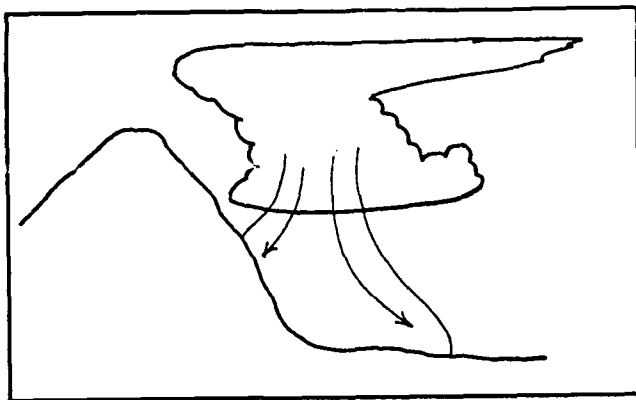


**Figure 3.11 Thunderstorm Formed Over Mountains.** When thunderstorms form over mountain slopes, the outflow is directed downslope. The additional force of gravity can produce violent winds.

Whenever moist low-level flow is directed into a substantial terrain barrier, condensation results when the low-level air flows far enough upslope to reach the LCL. Free convection takes place when the air is forced to the LFC. The terrain barrier only provides the triggering mechanism--the same basic ingredients (instability and moisture) as for any thunderstorm are also required--see Figure 3.12.

Differential surface heating can also provide a trigger. On a calm, clear day, mountain tops get direct solar heating before the valleys. When the air is heated, a slight hydrostatic imbalance is created, resulting in weak flow up the mountain sides (the valley breeze). Upslope flows from both sides converge at the peak and upward motion continues. If the air is unstable, thunderstorms form over peaks and ridges, as shown in Figure 3.13. This effect can be seen by comparing morning and

afternoon visible satellite imagery. If upper-level winds are strong enough, these storms move off the mountains and over adjacent areas. This type of convection is highly diurnal.

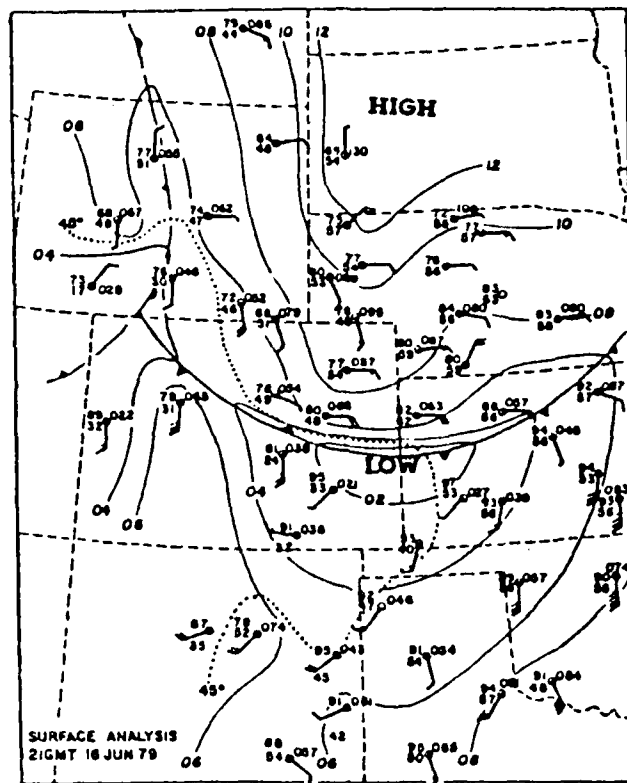


**Figure 3.12 Synoptic-Scale Easterly Flow into the Rockies Results in Significant Orographic Lift.** In this case, flow behind the front produced severe thunderstorms along the eastern slopes of the Rockies (Doswell, 1982).

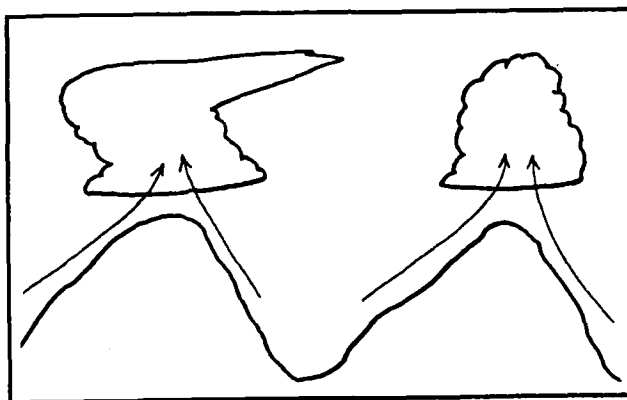


**Figure 3.13 Differential Heating on Mountain Tops Results in Valley Breezes Converging at the Peaks.** If the air is unstable, thunderstorms frequently result.

# THE SEVERE THUNDERSTORM

**4.1 General.** Severe thunderstorms are different creatures than their ordinary, "garden variety" counterparts. Although all thunderstorms have similar life cycles, certain conditions must be met before they become producers of severe weather. Forecasters must be familiar with these conditions before they attempt to decide whether or not the situation at hand will produce severe thunderstorms, or just general convective activity.

Any thunderstorm is usually capable of producing a brief "one-shot" episode of severe weather. With the exception of the "pulse storm" described in 4.5, this section will discuss the organized and persistent thunderstorms that produce persistent or recurring episodes of severe weather. Excluding the effects of lightning, these storms produce nearly all thunderstorm-related damage, injury, and death.

**4.2 Multicell Severe Thunderstorms.** The first requirement for a thunderstorm to achieve severe potential is the degree of instability that will allow the formation of a more powerful updraft. By itself, this is

not enough to produce a severe thunderstorm, at least not one that lasts for very long. The cell must be allowed to survive long enough to produce and sustain severe weather. The premature death of a thunderstorm is usually caused by updraft collapse due to downdraft interaction.

To keep a storm alive, the updraft must remain active and unimpeded. Hydrometeors (water droplets and frozen particles) forming in the middle and upper portions of the updraft core must not fall back through the updraft. If strong mid-level winds are present at 20,000 to 30,000 feet, they carry the hydrometeors so far downstream that they do not fall into the updraft. A downdraft (completely separate from the updraft) forms in conjunction with the precipitation in the forward portion of the storm, as shown in Figure 4.1. In addition to being cleared of obstructions, the updraft intensifies beneath mid-level winds as it draws mass from below through an action similar to the suction effect of a paint sprayer.

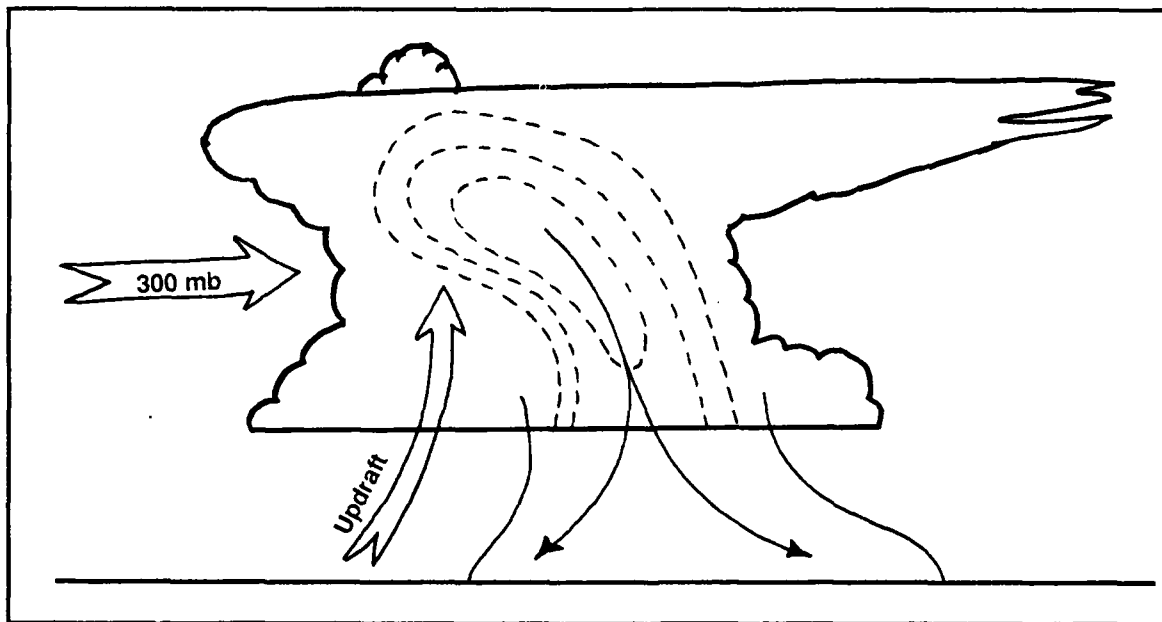


**Figure 4.1** Strong Winds Aloft Carry Precipitation Downstream. A downdraft is created in the forward flank of the storm where it does not interfere with the updraft. Dashed lines represent radar reflectivity.

With the updraft increasing in intensity, the storm grows larger. The momentum of the high-speed updraft carries mass far above the EL (sometimes by several thousand feet), resulting in a cumuliform dome that overshoots the cirrus anvil deck. At lower levels, the inflow is blocked from entering at the front of the storm

by the rainy downdraft and its associated outflow. The presence of southerly low-level winds results in the storm drawing air from its right flank. This allows the swelling cell to take advantage of the warm, moist flow that can help force the updraft from below--see Figure 4.2.

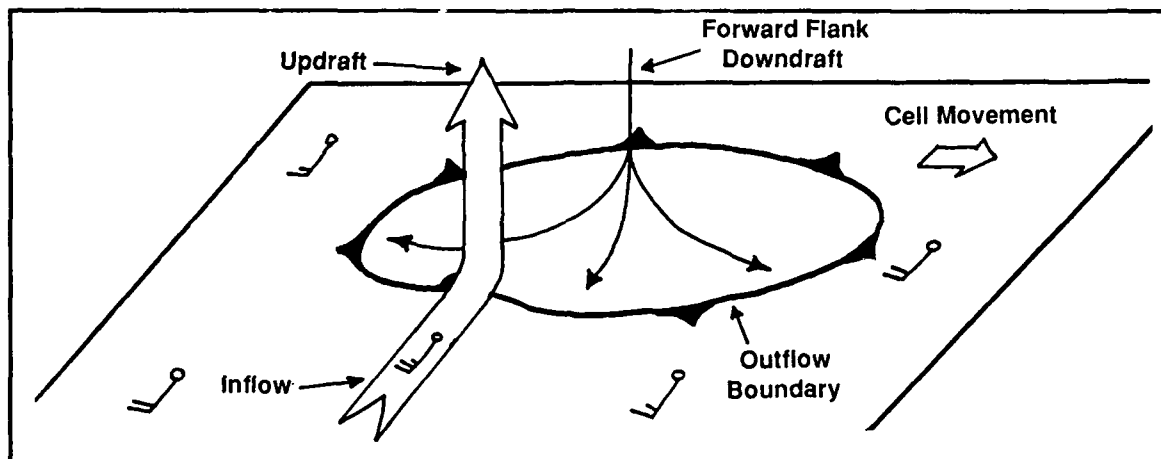


**Figure 4.2** Bubble of Outflow Air Blocks Inflow from Front of Storm. Low-level flow force-feeds the storm from its right flank.

Because it is dynamically supported from above and below, the updraft is strong enough to push the hydrometeors up and out of its way. This creates a cavity on the right flank of the storm (relative to storm motion) that is observable on radar as a "weak echo

region," or WER. Figure 4.3 shows typical development of a multicellular thunderstorm complex. Notice (in Figure 4.3c) how the mid-level echo overhangs the WER on the right flank.

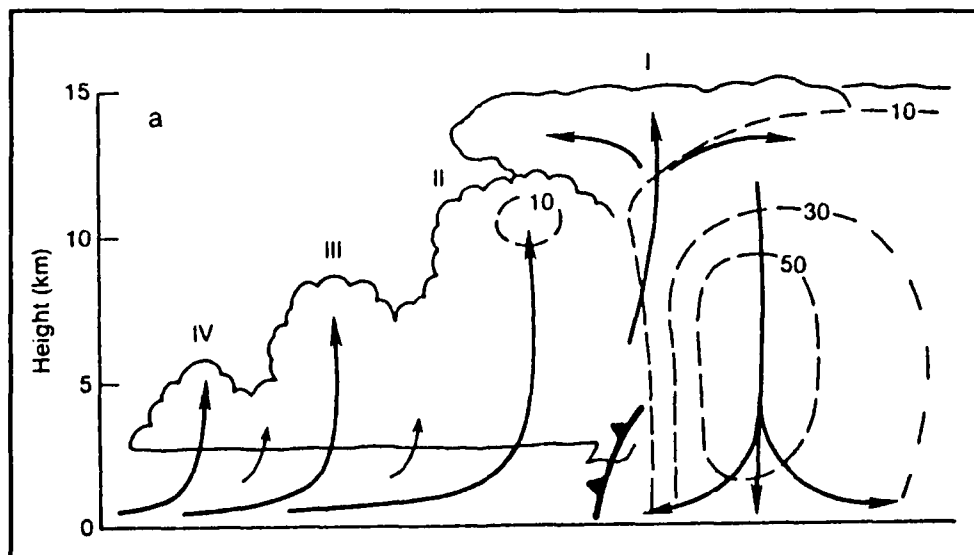


**Figure 4.3a** A Multicellular Thunderstorm Complex. Developing cells I, II, III, and IV are shown from right to left. Updrafts and downdrafts are shown by the flow lines. Dashed lines represent radar reflectivity (From Doswell, 1985).

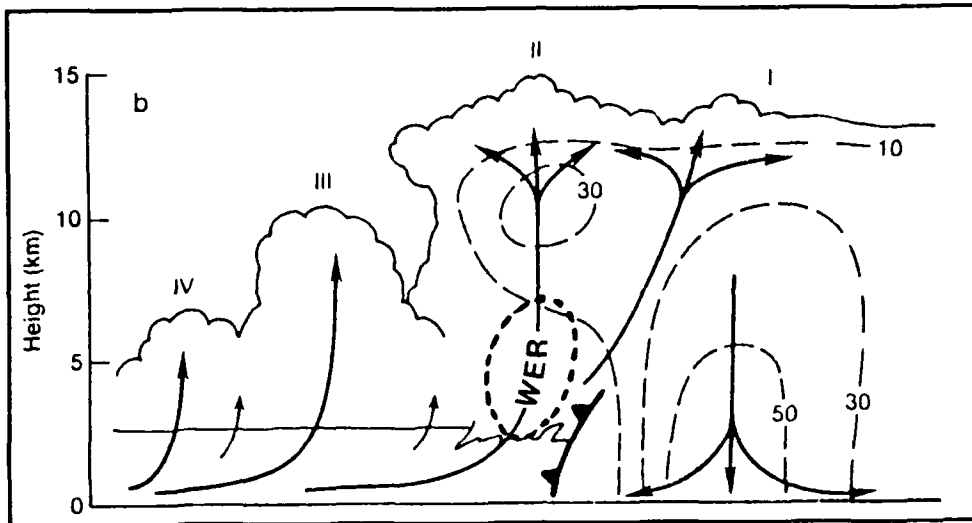


**Figure 4.3b A Multicellular Thunderstorm Complex Plus 10 Minutes.** The cells in 4.3a are shown here 10 minutes later. Updrafts and downdrafts are shown by the flow lines. Dashed lines represent radar reflectivity (From Doswell, 1985).

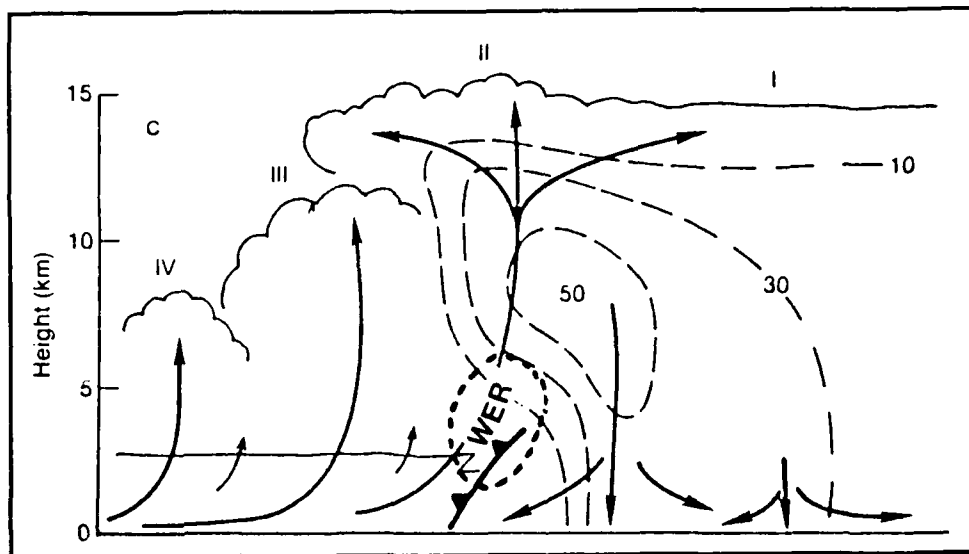


**Figure 4.3c A Multicellular Thunderstorm Complex Plus 20 Minutes.** Updrafts and downdrafts are shown by the flow lines. Dashed lines represent radar reflectivity. Note the presence of the WER. (From Doswell, 1985).

When the updraft reaches the intensity shown in Figure 4.3c, it is capable of producing 3/4-inch hailstones. The largest hail will fall just to the left and downstream of the updraft core, relative to storm motion. The largest stones will fall out (or through) the updraft first, while the smaller ones are carried farther

downstream by the strong winds aloft. Contrary to popular belief, the largest hail rarely falls in the heaviest radar echo region or area of heaviest precipitation, but near the inflow edge of the low-level radar echo. Figure 4.4 shows typical hail distribution.



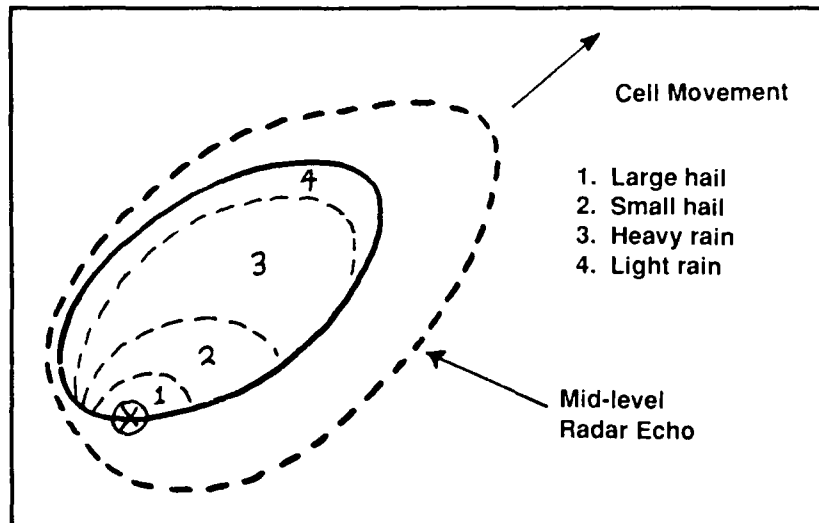


**Figure 4.4** *Precipitation Distribution in a Multicellular Thunderstorm.* The solid oval represents the low-level radar echo; the larger dashed oval, the mid-level radar echo. The circled "X" is the maximum echo top, or updraft core. Precipitation distribution areas are as indicated.

When the outflow from the rainy downdraft pushes against the inflow on the right flank, low-level convergence and lifting occurs. This is a favored location for new cell development. Often, a line of increasingly larger cumulus towers are observed building into the right flank of the storm. These flanking line cells eventually merge with the parent thunderstorm cell, as was shown in Figure 4.3. When new cells continue to form on the right flank and develop into mature storms,

they give the impression that the storm is travelling somewhat to the right of its expected path--see Figure 4.5. This effect (redevelopment or propagation) has long been considered a radar indication of possible severe weather. Individual cells generally move with the winds aloft. As older cells move downstream, newer ones take their place. The result is that there is always more than one cell in existence at a time in the storm complex--hence, the multicell severe thunderstorm.

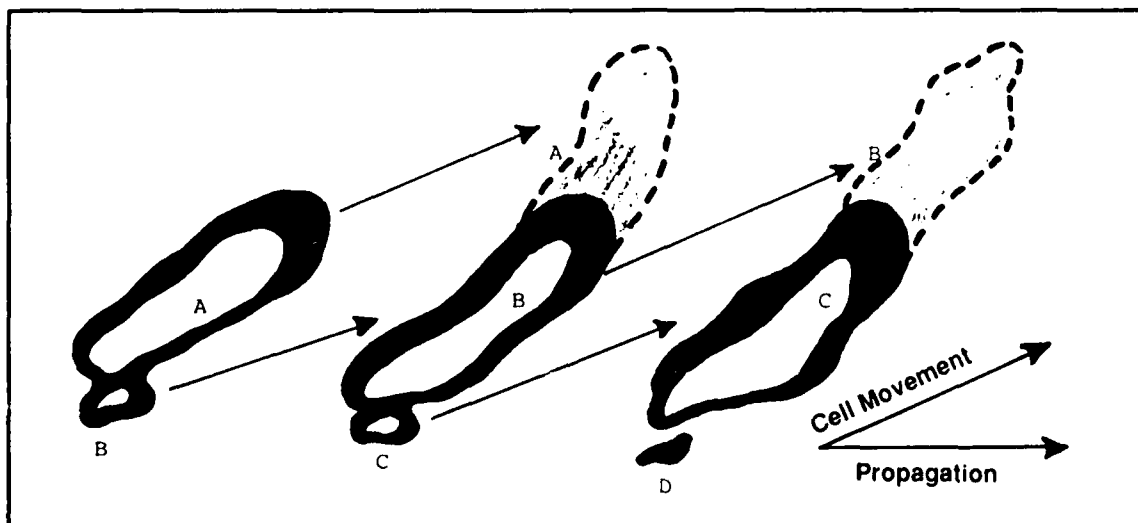


**Figure 4.5** *Radar View of New Cell Regeneration in a Multicell Complex.* New cells form on the right flank, move through the complex, and dissipate on the left flank. This gives the impression that the complex is moving to the right.

**4.3 Supercell Thunderstorms.** If the atmosphere is extremely unstable and the wind configuration favorable, the updraft can intensify still further. The ideal situation would be for winds to increase and veer with height. We have already seen (in 4.2) the effect strong winds aloft have on sustaining the updraft. A strongly sheared wind environment also contributes to separating the updraft and downdraft and to strengthening the storm. With southerly winds at the lower levels and westerly winds at higher levels, strong differential thermal advection takes place. Southerly winds transport warm moist air into the lower storm environment, while westerly winds transport cooler, and often drier, air aloft. This kind of differential advection serves to further destabilize the environment while maintaining the unstable conditions. Investigations by Marwitz (1972) and Doswell and Lemon (1979) show that pronounced veering (50 degrees) in the subcloud layer (surface to cloud base) appears to be critical for creating a supercell from a multicell system. They also found that supercell subcloud wind speeds were higher (at 10 m/sec) than the 8 m/sec found in multicell systems. Marwitz concluded that the conditions essential to supercell formation were veering winds with height and 10 m/sec wind speeds in the subcloud layer. The dynamic reasoning for this is elusive, but it is conceivable that the strong subcloud winds act to force the updraft by ramming warm, moist air into the inflow flank of the storm. The reader is directed to the numerical modeling efforts of Weisman and Klemp (1986), which graphically illustrate the effects of different vertical wind profiles on convective-scale development.

As the updraft intensifies further, it becomes more upright than in lesser thunderstorms because it is now strong enough to overcome the shearing effects of upper-level winds. So much mass is carried aloft by the updraft that it diverges rapidly at the EL, often causing the anvil to grow rapidly in all directions, even upstream against the upper-level winds. This creates a sharp, backsheared (upwind) anvil edge that is easily recognizable in satellite imagery. To compensate for all the mass being forced aloft, subsidence takes place outside the cloud, resulting in the suppression of surrounding convective activity. Any nearby convective cells are eventually obliterated as the dominant cell starves them of their warm, moist air to feed its own voracious

updraft. The result is one powerful cell in control of its environment--the supercell. Because of the dynamic support that the updraft receives and the constant resupply of unstable air, a supercell can persist for several hours.

The intense updraft causes a change in the configuration of the WER. Because of the high speeds, precipitation forms higher within the updraft and results in the creation of a cavity in the mid-level radar echo overhang. The WER now extends into the mid-level overhang, creating what is known as a "bounded weak echo region," or BWER--see Figures 4.6a. and b. The updraft region is "bounded" by higher radar returns and is indicative of a very strong updraft. An updraft of this magnitude can produce even larger hailstones than a multicell updraft, and the "steadier state" of the supercell results in a longer hail swath at the surface. The location of the largest hailfall is similar to the multicell case shown in Figure 4.4.

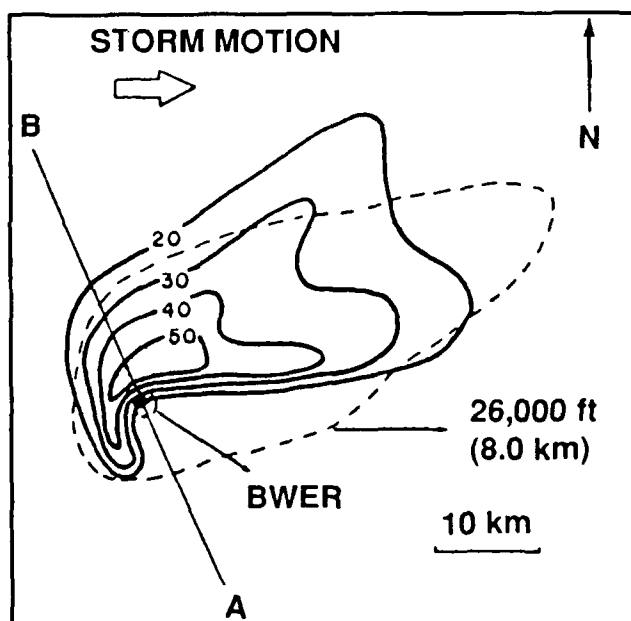


*Figure 4.6a Horizontal (PPI) Radar View of a Supercell.* Solid lines represent low-level reflectivity, while dashed lines represent the extent of the mid-level echo. Solid lines indicate the plane of the cross-section in Figure 4.6b (From Lemon, 1980).

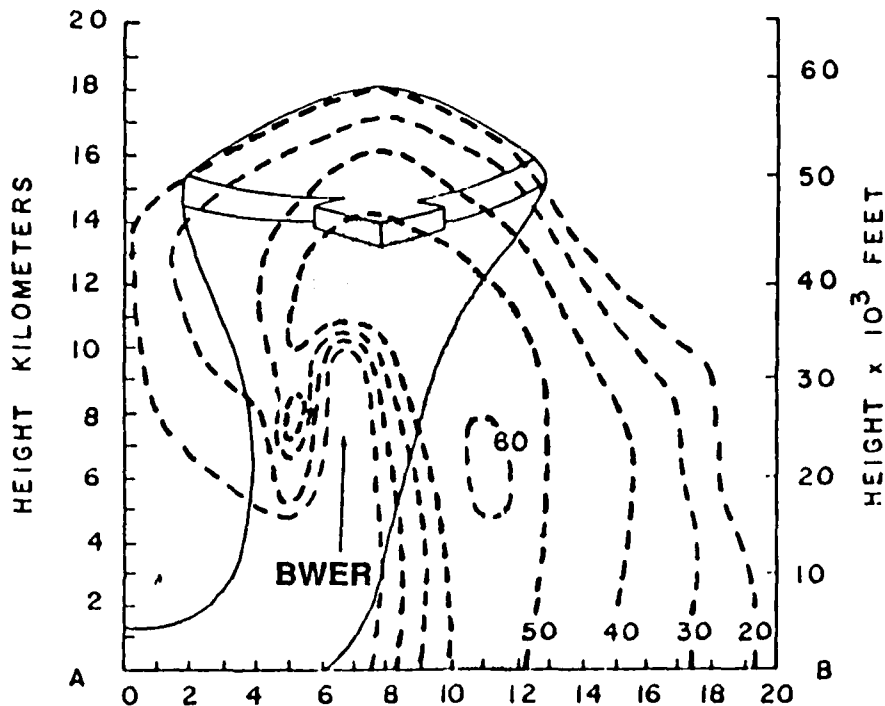


**Figure 4.6b** Vertical (RHI) Radar View of a Supercell. Dashed lines represent reflectivity (From Lemon, 1980).

The updrafts in supercell thunderstorms almost always rotate about a vertical axis. The source of rotation is still debated, but the most popular theory involves the tilting of vorticity fields, a principle illustrated in Figure 4.7. Along the outflow boundary, strong anticyclonic shear is produced between inflow and outflow. The horizontal roll cloud that often forms ahead of strong thunderstorms is vivid evidence that this shear exists. Along the right flank of the thunderstorm cell, some of this shear may be drawn into the intense updraft.

When the anticyclonic vorticity field is tilted upward, it is oriented about a vertical axis and, if viewed from above, is cyclonic. The updraft is then induced to rotate cyclonically about a vertical axis and, if stretched in the vertical, rotates faster. The rotating updraft is referred to as the mesocyclone in its "organizing stage." This scenario is quite possible, without the presence of an outflow boundary, in areas where wind speeds increase rapidly above the surface to produce vertical speed shear.

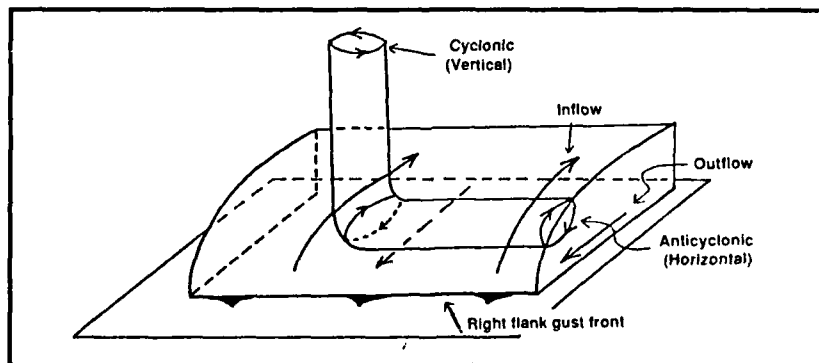


**Figure 4.7** Three-Dimensional Representation of the Right Flank Outflow Boundary (Gust Front). Vertical shear along the boundary interface results in anticyclonic vorticity about a horizontal axis. The updraft entrains this air, tilting it upward. The vorticity is transformed to cyclonic about a vertical axis, inducing the updraft to rotate cyclonically.

The rotation of the updraft has a pronounced effect on the structure and behavior of a supercell. The circulation pulls precipitation around the backside of the updraft core, creating a pendant-like protrusion on the right rear quadrant of the low-level radar echo--see Figure 4.8.

The strong swirling inflow draws warm and moist surface air upward, resulting in a lower condensation level (and therefore a lower cloud base) where the inflow (updraft) enters the cloud base. This feature, known as a "wall cloud," frequently shows rotation. At this stage, the updraft is at its maximum strength. The storm top is at its highest extent, directly over the updraft core. Hail is at its largest, falling to the left and somewhat ahead of the wall cloud--see Figure 4.9. Funnel clouds are common, and weak tornadoes may touch down briefly.

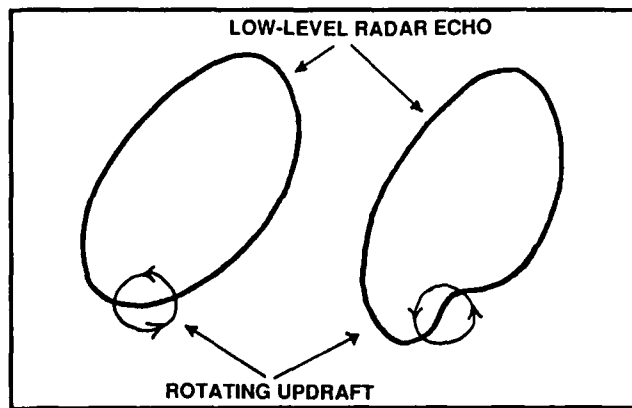


Figure 4.8 Rotating Updraft in Right Rear Flank Deforms Low-Level Radar Echo into Pendant Shape.

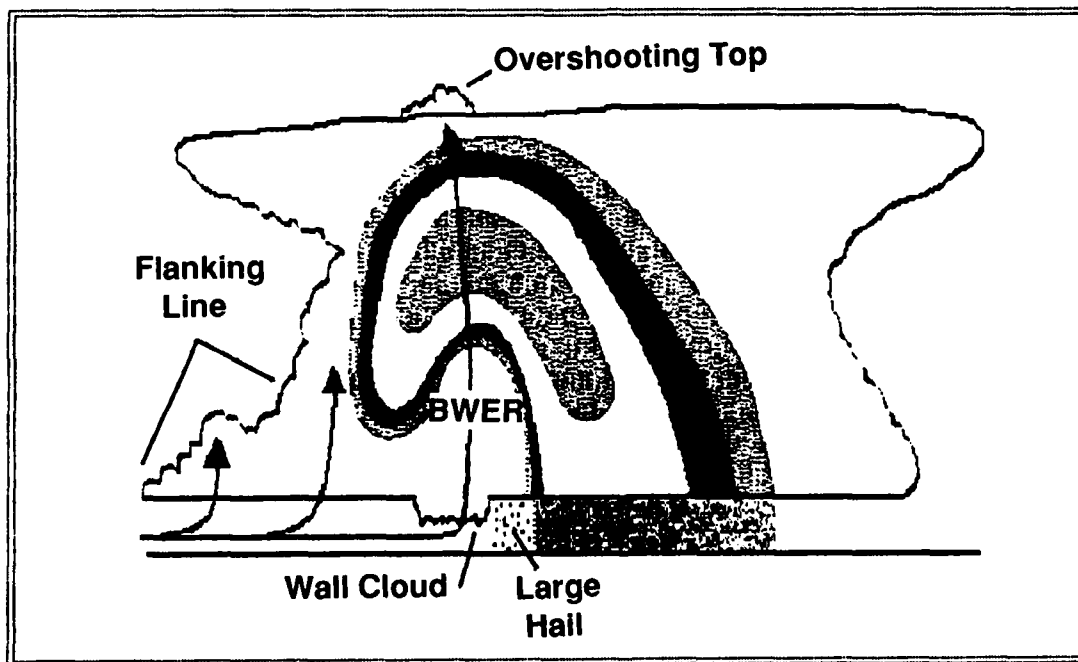
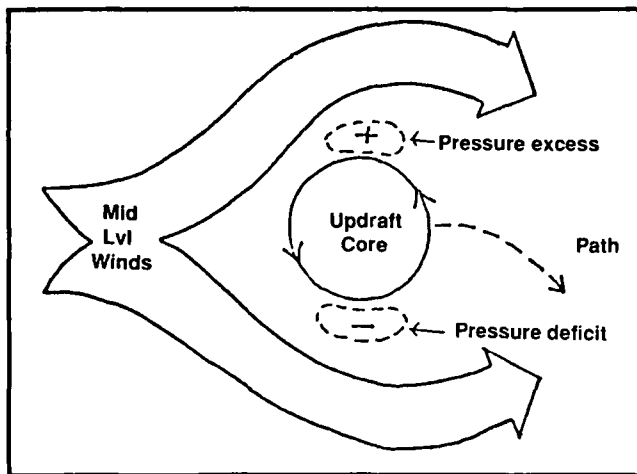


Figure 4.9 Vertical Cross-Section of an Adult Supercell. Note the location of the wall cloud with respect to the updraft and the BWER. Largest hail characteristically falls to the left of the wall cloud (relative to storm motion) on or near the reflectivity gradient. Funnel clouds are common with the wall cloud. Stippled areas represent radar reflectivity, looking west.

In the mid-levels of the storm, the rotating updraft effectively obstructs horizontal wind flow. As the winds split around the rotating updraft core, they converge with the circulation on the left side, resulting in a mass buildup and a subsequent pressure excess to the left of the updraft core. On the right side, they travel with each other, resulting in a relative pressure deficit. In order to correct the pressure imbalance, the updraft core is forced

to shift to the right, toward lower pressure. Where the updraft goes, the storm must follow. The result is a supercell that deviates to the right of the mean upper-level wind flow, as shown in Figure 4.10. This principle of fluid dynamics is termed the "Magnus Effect" (Fujita, 1965). It offers one explanation for the deviant movement of supercells.



**Figure 4.10 A Supercell Deviates to the Right of Mean Upper-Level Flow.** As upper flow splits around the rotating updraft, a pressure imbalance is created. This forces the updraft core to deviate to the right of the original path (dashed arrow) and causes the storm to move to the right of the upper winds.

Pressure increases under the upwind edge of the anvil when strong mid-level flow piles up against the rear of a rotating updraft core. As the mass increases, subsidence begins. The subsidence is enhanced by the evaporational cooling that takes place when drier mid-level air erodes the backside of the storm cloud. Subsidence tends to channel mid-level flow downward, creating a dynamic downdraft in the rear of the storm, as shown in Figure 4.11a. This "rear flank downdraft" (RFD) is in addition to a precipitation-induced "forward flank downdraft" (FFD).

As the RFD intensifies, it begins to deform the updraft, and a cyclonic shear zone forms at the updraft/RFD interface in the middle levels of the storm--see Figure 4.11b. At this stage, the mesocyclone center moves near the interface and is divided between the updraft and the RFD. It's usually evident in the radial velocity display of Doppler radar as a tight positive/negative velocity gradient.

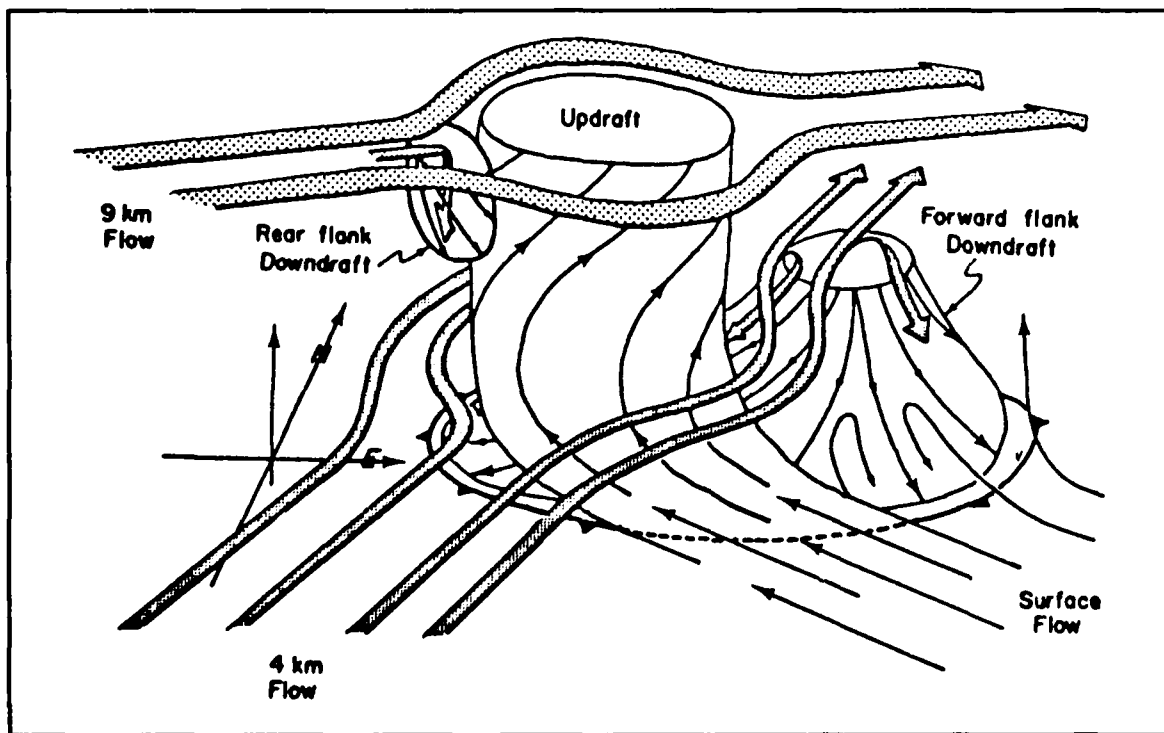


**Figure 4.11a Three-Dimensional Airflow Schematic in a Supercell--Initiation of RFD.** The initiation of the RFD is shown as the mid-level winds converge against the intense updraft core (From Lemon and Doswell, 1979).

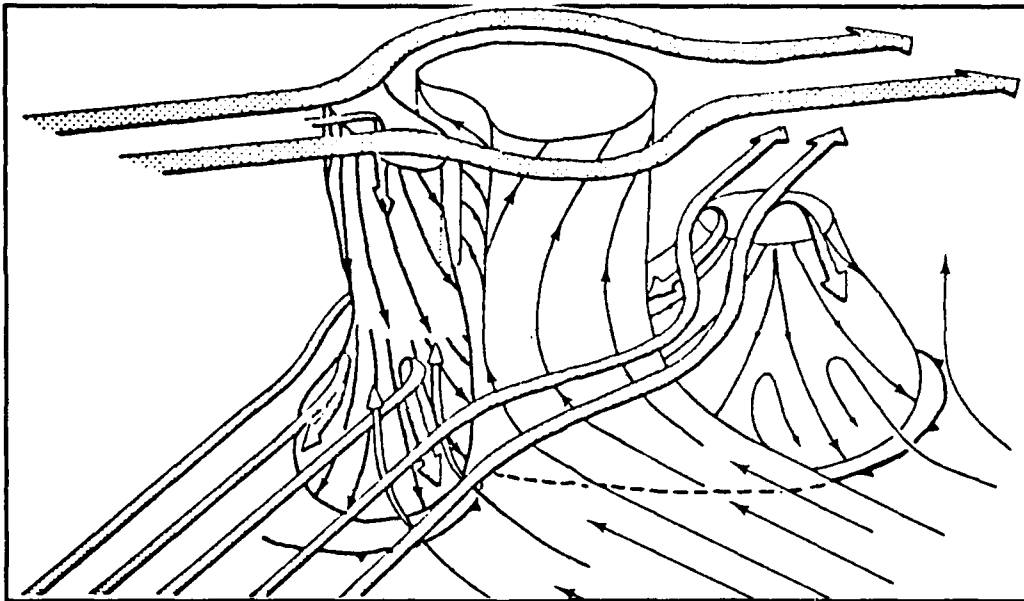


**Figure 4.11b Three-Dimensional Airflow Schematic in a Supercell--RFD Reaches the Surface.** The RFD reaches the surface and spreads out as a new air mass. The interaction of the updraft and RFD creates a circulation center in the mid levels (mesocyclone) (from Lemon and Doswell, 1979).

As the RFD gains strength, the mesocyclone (now in its mature stage) extends through a deep layer as it is stretched downward. The vertical stretching results in further intensification and a decrease in diameter. This small, intense velocity gradient is called the "tornado vortex signature," or TVS. As the RFD reaches the

surface and spreads out and around the right side of the updraft (the updraft circulation offers the least resistance on its right side), the RFD air advances eastward as a new gust front--see Figure 4.11c . The mesocyclonic circulation is pulled down by the RFD until it reaches the surface as a tornado.

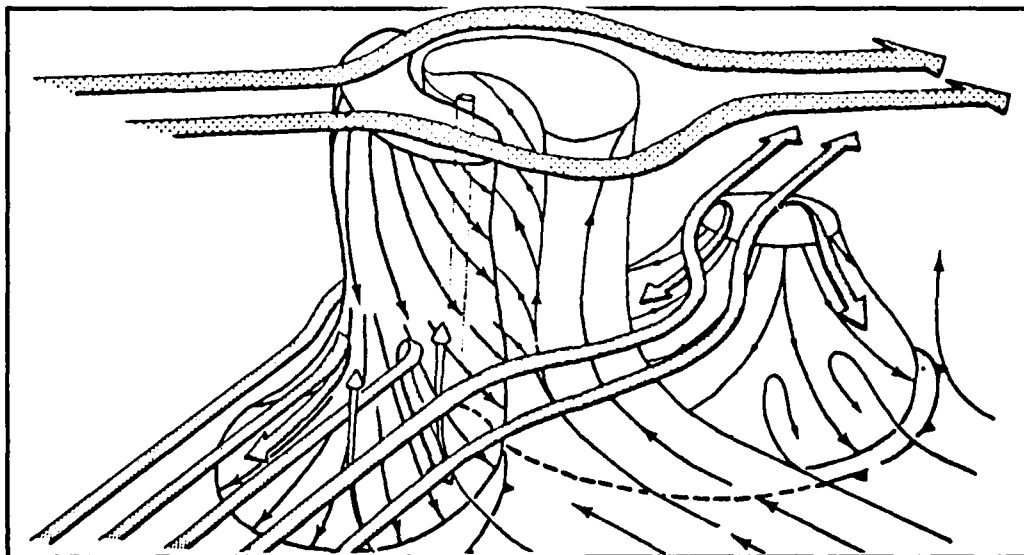


**Figure 4.11c Three-Dimensional Airflow Schematic in a Supercell--The RFD Strengthens.** As the RFD strengthens, the mesocyclone is pulled down to the surface where a tornado develops in the shear zone between inflow and outflow (from Lemon and Doswell, 1979).

As the RFD continues to spread, the low-level pendant is deformed into the more familiar hook shape (Figure 4.11d). The hook itself is precipitation caught in the advancing RFD air, and may contain damaging straight-line winds. The open, or echo free, area is the

updraft core (the BWER in the horizontal plane). The tornado is typically found on the interface between the RFD and the updraft, which is a strong cyclonic shear zone near the tip of the hook.

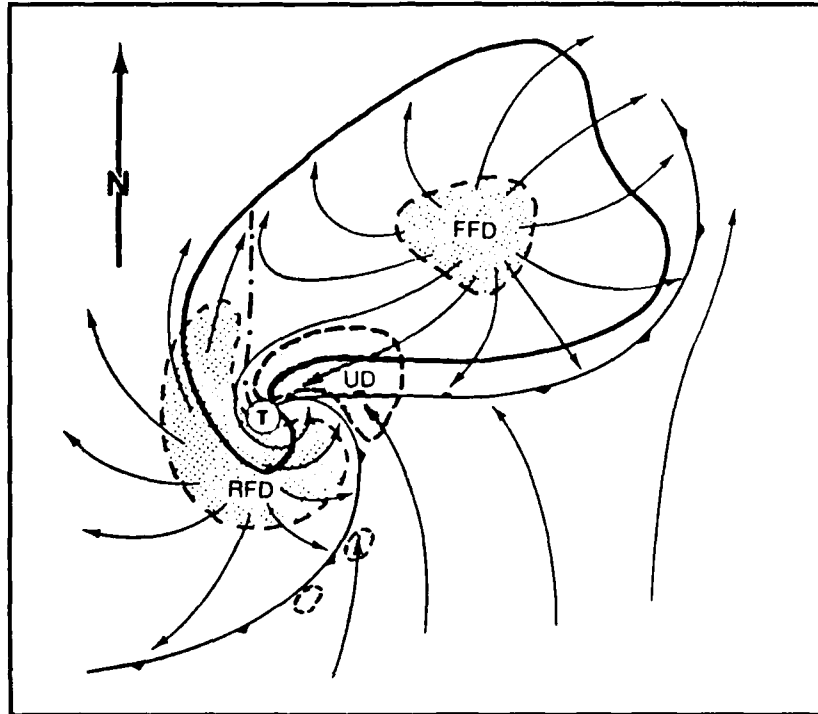


**Figure 4.11d Low-level Airflow Schematic in a Tornado-Producing Supercell.** The solid outline represents the low-level radar echo (notice the hook on the right rear quadrant). The tornado (T) is on the interface between inflow and outflow (from Lemon and Doswell, 1979).

The action of the RFD eventually takes its toll on the updraft. As the updraft weakens due to the drag of the RFD, there is a drop in the storm top. This is consistent with Lemon's findings (1980) of BWER collapse at the time of major tornado production. Eventually the updraft collapses entirely under the domination of the RFD;

when it does, tornado activity stops. The RFD vs. updraft battle, however, may go on for hours, producing long-track tornadoes. A new updraft may form at the occlusion of the storm-scale fronts, and the cycle shown in this series of figures begins again--see Figure 4.11c.

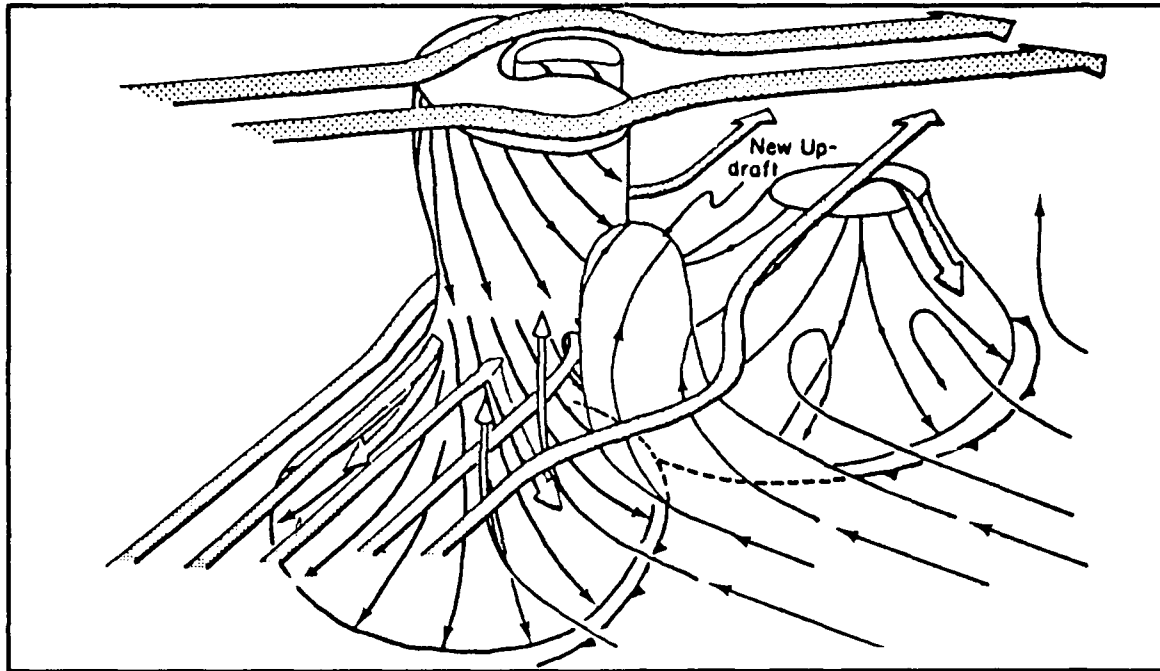


**Figure 4-11e Three-Dimensional Airflow Schematic in a Supercell--The Updraft Collapses.** The RFD weakens and collapses the updraft as the tornado dissipates. A new updraft may form.

Figure 4.12 is a look-down view of a supercell thunderstorm, showing the distribution of associated surface weather. If one considers the approach of the storm from the west-southwest, this model is consistent with eyewitness observations of increasing hail size followed by a dead calm just before the tornado strikes.

The calm condition, which does not always occur, results from the col created at the surface where the horizontal flow becomes vertical as it enters the updraft beneath the wall cloud. The author experienced this effect while standing beneath a supercell updraft in central Iowa on 23 May 1981.

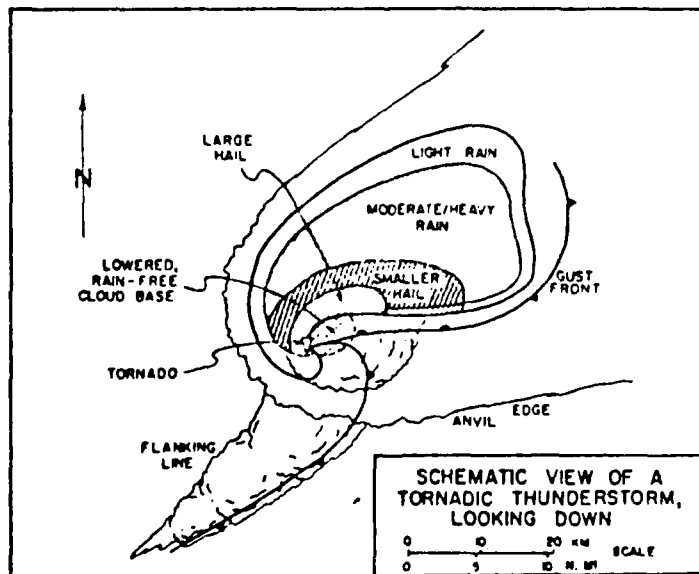


**Figure 4.12 Look-Down View of a Tornadoic Thunderstorm, Showing Observed Features.** Note the presence of large hail in advance of the tornado area (from Lemon, 1979).



**4.4 Squall Lines.** The squall line (introduced in 3.3) is an organized line of thunderstorm cells that commonly forms in advance of a fast-moving cold front--an example is shown in Figures 4.13a and b. Squall lines can produce severe weather, most frequently in the form of strong straight-line winds. Squall lines can also produce hail and tornadoes, but normally only when one of its cells attains multicell or supercell status.

As thunderstorms begin to develop in the low-level convergence zone ahead of the front, the downslope flow along the frontal surface injects dry air into the rear of the cells. Evaporational cooling occurs as the dry air mixes with the moist in-cloud air. This affects the thunderstorms in two ways: First, mid-level cooling further destabilizes the immediate thunderstorm environment, giving the updraft more thermal support. Second, the evaporationally cooled air subsides and provides a means for the mid-level flow to be transferred downward to the surface, as shown in Figure 4.13b. If the mid-level winds are strong, this dynamic downrush can be violent. The downrush air spreads out into a long gust front at the leading edge of the squall line. Frequently, a shelf or horizontal roll cloud is observed along the advancing gust front. As the downrush gust front rushes ahead, it provides a lifting mechanism that generates new cells ahead of the parent squall line. This allows the line to propagate normal to the front while the individual cells travel parallel to the line, with upper-level flow.

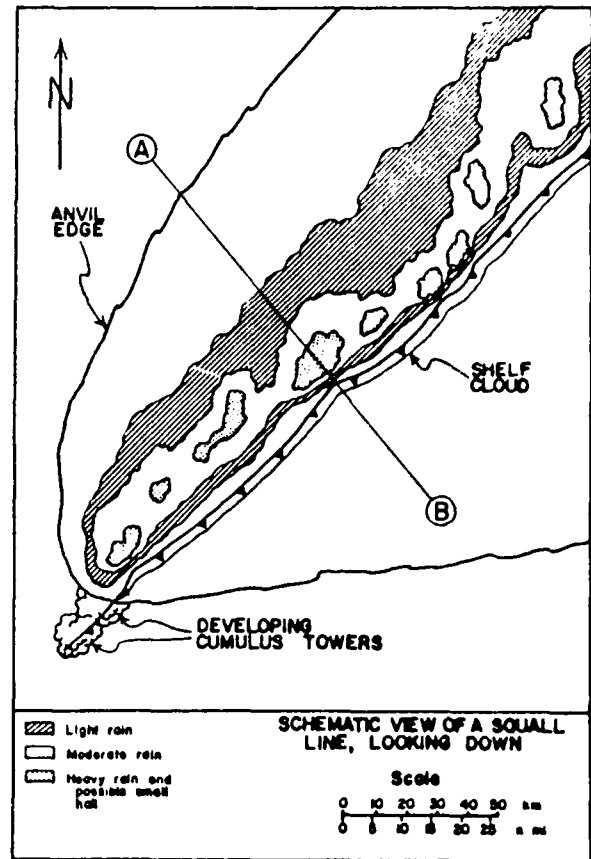


*Figure 4.13a Vertical (Look-Down) View of Squall Line.* Line A-B corresponds with line A-B in Figure 4-13b (from Doswell, 1985).

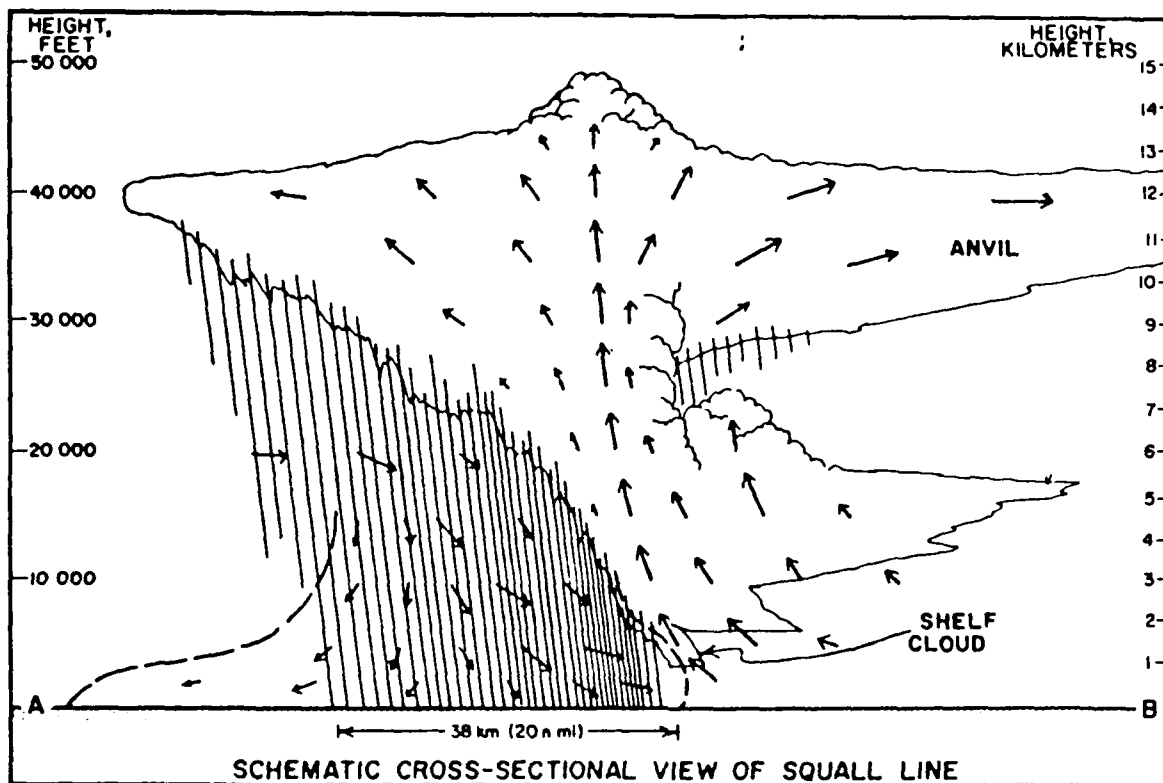


Figure 4.13b Cross-Sectional (Side) View of Squall Line (Doswell, 1985).

Since flanking cells prevent inflow from any other direction, squall line thunderstorms tend to draw inflow from their forward flanks. As a result, individual cells compete for low-level moist air and make it difficult for any one cell to intensify at the expense of the others. This is especially true when the squall line is more or less solid as viewed by radar. If the line is broken, however, with large spaces between cells, they may develop independently without interference from other cells. In this case, the probability of severe weather production, other than straight-line wind, increases. The cell at the tail (upwind) end of the line is also a probable severe weather producer. This cell, besides being the newest, has the capability of drawing totally undisturbed warm, moist air into its right flank. It normally assumes multicell, sometimes supercell, proportions if environmental conditions are otherwise conducive to such growth.

**4.5 Pulse-Severe Thunderstorms.** Nearly every forecaster has seen the ordinary-looking thunderstorm that, for no apparent reason, suddenly produces severe weather. By the time a warning is issued, the event is

over and never occurs again. This is the nature of the "pulse-severe" storm. The name implies its "one shot" severe weather production methods. Pulse storms become severe through brief intensifications of the updraft. The precise reasons for this are not known, but it may be caused by an undetectable pocket of dry air that finds its way into the cell.

There is, however, a way to detect a potential pulse storm. Investigators (Wilk, et al, 1979) found that the pulse storm develops its first radar echo at a higher level (7-9 km) than non-severe storms (3-6 km). Pulse storms contain a high reflectivity core that extends to greater heights, persists longer, and maintains continuity as it descends to the surface. If the 50 dBZ core reaches or exceeds 9 km (29,500 feet), the probability of a severe weather event is very high. If large hail occurs, it will be found in the 50 dBZ core as it reaches the surface.

Figure 4.14 is the vertical depiction of a pulse storm compared to a non-severe storm. Detection requires constant monitoring of radar and comparison of suspect cells with surrounding cells.

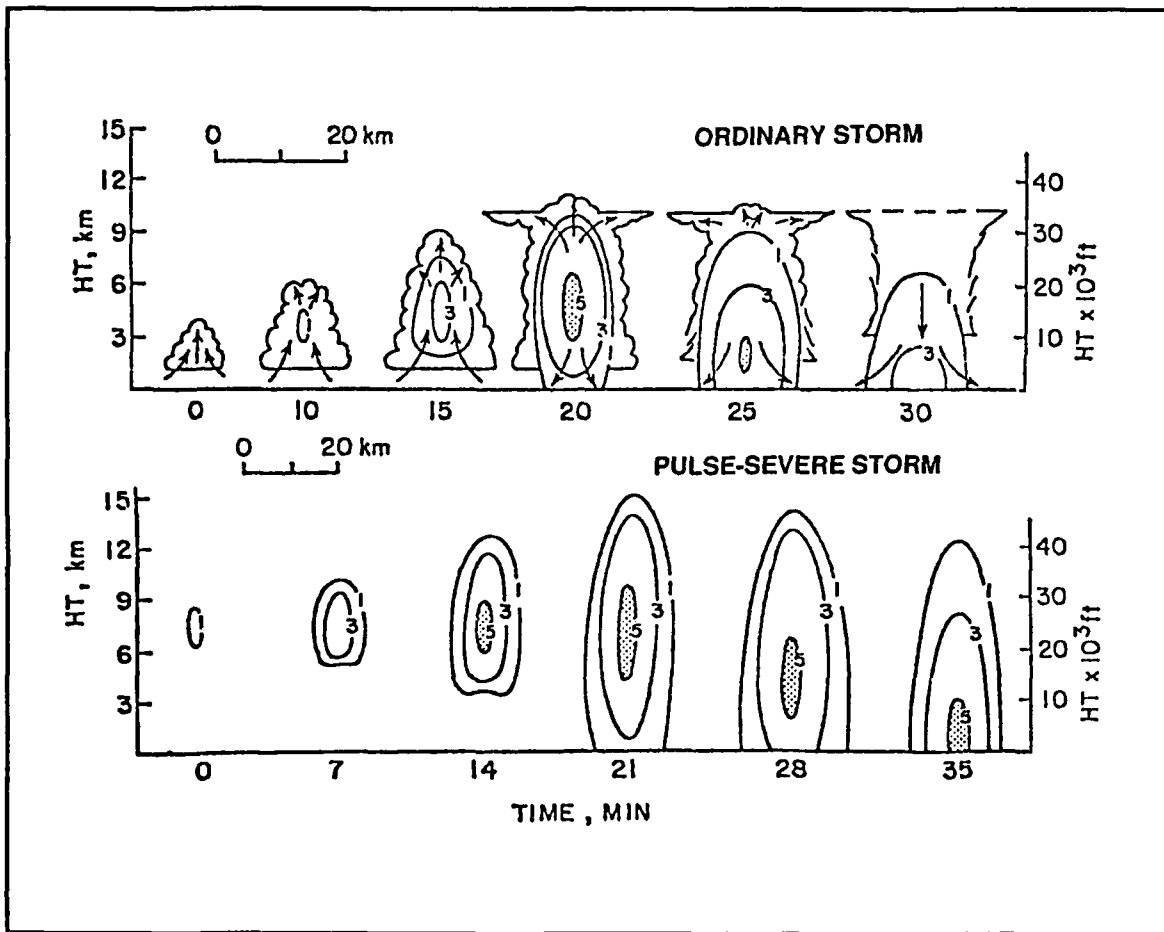


**Figure 4.14 Radar Depiction: Evolution of an Ordinary Thunderstorm (top), and a Pulse Storm (bottom).** Solid lines represent radar reflectivity. Notice that the VIP 5 (50 dBZ) core in the pulse storm is found at a much higher level than in the ordinary storm. The VIP core also maintains continuity with descent to the surface (after Wilk, et al., 1978).

**4.6 Downbursts.** The downburst is not a type of thunderstorm, but a severe weather event. It is simply an extremely powerful downrush from a convective cell. Downbursts strike the ground and spread rapidly outward as damaging horizontal winds. They may be "one shot" episodes, or they may persist along a long track, as shown in Figure 4.15. Downbursts commonly occur with sharply bulging, or bowing, thunderstorm lines.

Fujita (1978) refers to these configurations on radar as "bow echoes"--see the examples in Figure 4.15. It appears that the downburst causes the bowing of the echo, rather than the other way around. For this reason, downburst detection is often very difficult until well into its life. Maximum downburst activity is normally found near the apex of the bow, at the leading edge of the storm.

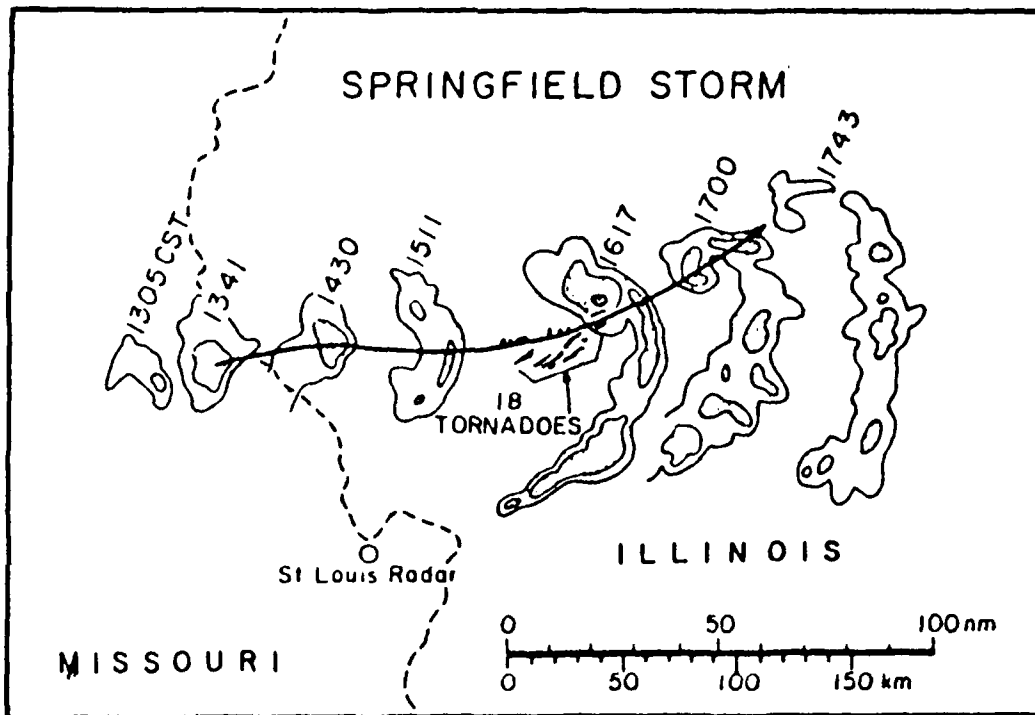


**Figure 4.15 Radar Depiction: The Life of a Bow Echo on 6 August 1977.** The solid line indicates the track of the downburst. Notice that the downburst formed well before the echo began to bow. The downburst dissipated when the bow echo began to break up (from Fujita, 1978).

The downburst formation mechanism is not really understood at this time, but there is speculation that the entrainment of dry mid-level winds are involved in a way similar to the downrush mechanism in a squall line. In any case, once a downburst has materialized, the strong winds plow ahead and rapidly advance the thunderstorm line into its bow echo shape. The bow echo generally travels rapidly. The downburst normally stays active until the bow echo begins to break up as an organized echo system (Fujita, 1978).

RFD-induced downbursts are also common in the hook echoes of supercells. A tremendous amount of low-level shear is produced by the rapidly advancing downburst gust front. This shear is capable of producing

tornado-like vortices along the flanks of the gust front. These vortices, or "gustnadoes" (Doswell, 1985), are capable of producing tornado-like damage. They are virtually undetectable. They have no radar signature, and they occur sporadically, with short life spans.

Microbursts are small-scale downbursts. Although not usually as strong, microbursts and the associated low-level wind shear are extremely dangerous to aircraft. They are particularly troublesome because they often originate in smaller convective cells, making detection virtually impossible. The microburst formation mechanism is not well understood either, but dry air entrainment (hydrometeors falling into dry air) is believed to be a primary factor.

## SUMMARY

The foundation for successful severe weather forecasting lies with the understanding of the basic convective processes and the inner workings of convective storms. Too often, severe weather warnings are issued only on shape recognition, without any real understanding of the relationship to the severe weather event. Too many other warnings are issued only after reports of a visual sighting (often questionable) have been received. It does not take an expert to issue a tornado warning after being told that one is on the way.

We hope this report will provide the reader a better understanding of convective storms. Although it does not address *all* the tools (stability indices, for example) used in severe weather forecasting, it should have made it apparent why we use them. It should also be apparent that severe convective phenomena behave, for the most part, very logically. This knowledge, combined with the forecasting tools and real-time data now available, can produce the timely and accurate severe weather warnings necessary to save lives and protect resources.

## BIBLIOGRAPHY

- Browning, K. A., "The Evolution of Tornadoic Storms," *J. Atmos. Sci.*, 22, pp. 664-668, 1965.
- Byers, H. R., and R. R. Braham, Jr., *The Thunderstorm*, U.S. Government Printing Office, Washington, D.C., 1949.
- Doswell, C. A. III, *The Operational Meteorology of Convective Weather Vol I: Operational Mesoanalysis*, Report No. NOAA TM NWS NSSFC-5, National Severe Storms Forecast Center, Kansas City, MO, 1982.
- Doswell, C. A. III, *The Operational Meteorology of Convective Weather Vol. II: Storm Scale Analysis*, Report No. NOAA TM ERL ESG-15, Environmental Sciences Group, Boulder CO, 1985.
- Fawbush, E. J., R. C. Miller, and L. G. Starrett, "An Empirical Method of Forecasting Tornado Development," *Bull. Amer. Meteor. Soc.*, 32, 1-9, 1951.
- Fujita, T., "Results of detailed synoptic studies of squall lines," *Tellus*, 4, pp. 405-436, 1955.
- Fujita, T., "Formation and Steering Mechanisms of Tornado Cyclones and Associated Hook Echoes," *Mon. Wea. Rev.*, 93, 67-78, 1965.
- Fujita, T., *Manual of Downburst Identification for Project NIMROD*, SMRP Res. Paper No. 156, Univ. of Chicago, Chicago, IL, 1978.
- Gesser, F., *Severe Weather Test Part I: Theory*, AWS/FM-85-002, HQ Air Weather Service, Scott AFB, IL, 1985.
- Grebe, R., *An Outline of Severe Local Storms with the Morphology of Associated Radar Echoes*, NOAA TM NWS TC-1, National Weather Service Training Center, Kansas City, MO, 1982.
- Kessler, E., (Ed.), *Thunderstorm Morphology and Dynamics*, Univ. of Oklahoma Press, Norman, OK, 1985.
- Kinzer, G. D., *Cloud-to-Ground Lightning Versus Radar Reflectivity in Oklahoma Thunderstorms*, NOAA TM ERL NSSL-59, Norman OK, 1972.
- Lemon, L. R., "On improving National Weather Service severe thunderstorm and tornado warnings," *Preprints, 11th Conf. on Severe Local Storms, (Kansas City)*, Amer. Meteor. Soc., Boston, MA, pp. 569-572, 1979.
- Lemon, L. R., and C. A. Doswell III, "Severe thunderstorm evolution and mesocyclone structure as related to tornadogenesis," *Mon. Wea. Rev.*, 107, pp. 1184-1197, 1979.
- Lemon, L. R., *Severe Thunderstorm Radar Identification Techniques and Warning Criteria*, NOAA TM NWS NSSFC-3, National Weather Service, Kansas City, MO, 1980.
- Marwitz, J. D., "The structure and motion of severe hailstorms, Part I: Supercell storms," *J. Appl. Meteor.*, 11, pp. 166-179, 1972.
- Marwitz, J. D., "The structure and motion of severe hailstorms, Part II: Multicell storms," *J. Appl. Meteor.*, 11, pp. 180-188, 1972.
- Miller, R. C., *Notes on Analysis and Severe Storm Forecasting Procedures of the Air Force Global Weather Central*, AWS TR 200 (Rev), Air Weather Service, Scott AFB, IL, 1972.

- Purdom, J. F. W., "The development and evolution of deep convection," *Preprints, 11th Conf. on Severe Local Storms (Kansas City)*, Amer. Meteor. Soc., Boston, MA, pp. 143-150, 1979.
- Rogers, R.R., *A Short Course in Cloud Physics*, Peragmon Press, 1976.
- Rotunno, R., *Tornadoes and Tornadogenesis, Mesoscale Meteorology and Forecasting*, Amer. Meteor. Soc., Boston, MA, pp. 414-436, 1986.
- Saucier, W.J., *Principles of Meteorological Analysis*, University of Chicago Press, pp. 262-302, 1955.
- The Use of the Skew-T, Log P Diagram in Analysis and Forecasting*, AWS/TR-79/006, HQ Air Weather Service, Scott AFB, IL, 1979 (revised 1990).
- Weisman, M. L., and J. B. Klemp, *Characteristics of isolated convective storms, Mesoscale Meteorology and Forecasting*, Amer. Meteor. Soc., Boston, MA, pp. 331-358, 1986.
- Wilk, K. E., L. R. Lemon, and D. W. Burgess, *Interpretation of radar echoes from severe thunderstorms: A series of illustrations with extended captions*, Prepared for training FAA ARTCC Coordinators, National Severe Storms Laboratory, Norman, OK, 1978.

## DISTRIBUTION

AWS/DO, Scott AFB, IL 62225-5008.....	1
AWS/DOTM, Scott AFB, IL 62225-5008.....	1
AWS/XT, Scott AFB, IL 62225-5008.....	1
AWS/XTX, Scott AFB, IL 62225-5008.....	1
AWS/PM, Scott AFB, IL 62225-5008.....	1
OL A, HQ AWS, Buckley ANG Base, Aurora, CO 80011-9599.....	1
SD/CWDA, PO Box 92960, Los Angeles, CA 90009-2960.....	1
OL-K, HQ AWS, NEXRAD Opnl Support Facility, 1200 Westheimer Dr. Norman, OK 73069.....	1
OL-L, HQ AWS, Keesler AFB, MS 39534-5000.....	1
OL-M, HQ AWS, McClellan AFB, CA 95652-5609.....	1
Det 1, HQ AWS, Pentagon, Washington, DC 20330-6560.....	1
Det 2, HQ AWS, Pentagon, Washington, DC 20330-5054.....	2
Det 3, HQ AWS, PO Box 3430, Onizuka AFB, CA 94088-3430.....	1
Det 9, HQ AWS, PO Box 12297, Las Vegas, NV 89112-0297.....	1
1WW/DN, Hickam AFB, HI 96853-5000.....	3
11WS/DON, Elmendorf AFB, AK 99506-5000.....	11
20WS/DON, APO San Francisco 96328-5000.....	12
30WS/DON, APO San Francisco 96301-0420.....	16
2WW/DN, APO New York 09094-5000.....	3
7WS/DON, APO New York 09403-5000.....	30
28WS/DON, APO New York 09127-5000.....	10
31WS/DON, APO New York 09136-5000.....	20
3WW/DN, Offutt AFB, NE 68113-5000.....	3
9WS/DON, March AFB, CA 92518-5000.....	15
24WS/DON, Randolph AFB, TX 78150-5000.....	12
26WS/DON, Barksdale AFB, LA 71110-5002.....	18
4WW/DN, Peterson AFB, CO 80914-5000.....	12
2WS/DON, Andrews AFB, MD 20334-5000.....	20
5WW/DN, Langley AFB, VA 23665-5000.....	3
1WS/DON MacDill AFB, FL 33608-5000.....	2
3WS/DON, Shaw AFB, SC 29152-5000.....	15
5WS/DON, Ft McPherson, GA 30330-5000.....	20
25WS/DON, Bergstrom AFB, TX 78743-5000.....	15
AFGWC/SDSL, Offutt AFB, NE 68113-5000.....	6
USAFETAC, Scott AFB, IL 62225-5438.....	3
7WW/DN, Scott AFB, IL 62225-5008.....	7
6WS/DON Hurlburt Field, FL 32544-5000.....	6
15WS/DON, McGuire AFB, NJ 08641-5002.....	14
17WS/DON, Travis AFB, CA 94535-5986.....	14
3350 TCHTG/TTGU-W, Stop 62, Chanute AFB, IL 61868-5000.....	2
3395 TCHTG/TTKO, Keesler AFB, MS 39534-5000.....	2
AFIT/CIR, Wright-Patterson AFB, OH 45433-6583.....	1
AFCSA/SAGW, Washington, DC 20330-5000.....	1
NAVOCEANCOMDET, Federal Building, Asheville, NC 28801-2723.....	1
NAVOCEANCOMDET, Patuxent River NAS, MD 20670-5103.....	1
NAVOCEANCOMFAC, Stennis Space Ctr, MS 39529-5002.....	1
COMNAVOCEANCOM, Code N312, Stennis Space Ctr, MS 39529-5000.....	1
NAVOCEANO, Code 9220 (Tony Ortolano), Stennis Space Ctr, MS 39529-5001.....	1
NAVOCEANO, Code 4601 (Ms Loomis), Stennis Space Ctr, MS 39529-5001.....	1
FLENUMOCEANCEN, Monterey, CA 93943-5006.....	1



NOARL West, Monterey, CA 93943-5006 .....	1
Naval Research Laboratory, Code 4323, Washington, DC 20375.....	1
Naval Postgraduate School, Chinn, Dept of Meteorology, Code 63, Monterey, CA 93943-5000.....	1
Naval Eastern Oceanography Ctr, U117 McCady Bldg, NAS Norfolk, Norfolk, VA 23511-5000.....	1
Naval Western Oceanography Ctr, Box 113, Attn: Tech Library, Pearl Harbor, HI 96860-5000.....	1
Naval Oceanography Command Ctr, COMNAVMAR Box 12, FPO San Francisco, CA 96630-5000.....	1
Pacific Missile Test Center, Geophysics Division, Code 3253, Pt Mugu, CA 93042-5000.....	1
Dept of Commerce/NOAA/MASC, Library MC5 (Jean Bankhead), 325 Broadway, Boulder, CO 80303 .....	2
Federal Coordinator for Meteorology, Suite 300, 11426 Rockville Pike, Rockville, MD 20852 .....	1
NOAA Library-EOC4WSC4, Attn: ACQ, 6009 Executive Blvd, Rockville MD 20852.....	1
NOAA/NESDIS (Attn: Nancy Everson, E/RA22), World Weather Bldg, Rm 703, Washington, DC 20233 .....	1
NOAA/NESDIS (Attn: Capt Taylor), FB #4, Rm 0308, Suitland, MD 20746 .....	1
GL/LY, Hanscom AFB, MA 01731-5000 .....	1
GL Library, Attn: SULLR, Stop 29, Hanscom AFB, MA 01731-5000.....	1
Atmospheric Sciences Laboratory, Attn: SLCAS-AT-AB, Aberdeen Proving Grounds, MD 21005-5001 .....	1
Atmospheric Sciences Laboratory, White Sands Missile Range, NM 88002-5501 .....	1
U.S. Army Missilc Command, ATTN: AMSMI-RD-TE-T, Redstone Arsenal, AL 35898-5250.....	1
Technical Library, Dugway Proving Ground, Dugway, UT 84022-5000 .....	1
NWS W/OSD, Bldg SSM C-2 East-West Hwy, Silver Spring, MD 20910 .....	1
NWS Training Center, 617 Hardesty, Kansas City, MO 64124 .....	1
NCDC Library (D542X2), Federal Building, Asheville, NC 28801-2723 .....	1
DTIC-FDAC, Cameron Station, Alexandria, VA 22304-6145.....	2
NIST Pubs Production, Rm A-405, Admin Bldg, Gaithersburg, MD 20899 .....	1
JSOC/Weather, P.O. Box 70239, Fort Bragg, NC 28307-5000.....	1
75th RGR (Attn: SWO), Ft Benning GA 31905-5000.....	1
HQ 5th U.S. Army, AFKB-OP (SWO), Ft Sam Houston, TX 78234-7000 .....	1
AUL/LSE, Maxwell AFB, AL 36112-5564.....	1
AWSTL, Scott AFB, IL 62225-5438.....	100